HAL
open science

Passivity-based tracking control of multiconstraint complementarity Lagrangian systems

Irinel-Constantin Morarescu, Bernard Brogliato

To cite this version:

Irinel-Constantin Morarescu, Bernard Brogliato. Passivity-based tracking control of multiconstraint complementarity Lagrangian systems. [Research Report] RR-6483, INRIA. 2008, pp.35. inria-00266810v2

HAL Id: inria-00266810

https://inria.hal.science/inria-00266810v2

Submitted on 29 Apr 2008

HAL is a multi-disciplinary open access archive for the deposit and dissemination of scientific research documents, whether they are published or not. The documents may come from teaching and research institutions in France or abroad, or from public or private research centers.

L'archive ouverte pluridisciplinaire **HAL**, est destinée au dépôt et à la diffusion de documents scientifiques de niveau recherche, publiés ou non, émanant des établissements d'enseignement et de recherche français ou étrangers, des laboratoires publics ou privés.

INSTITUT NATIONAL DE RECHERCHE EN INFORMATIQUE ET EN AUTOMATIQUE

Passivity-based tracking control of multiconstraint complementarity Lagrangian systems

Irinel–Constantin Morărescu — Bernard Brogliato

N° 6483

Mars 2008

Thème NUM

Rapport de recherche

ISSN 0249-6399 ISRN INRIA/RR--6483--FR+ENG

INSTITUT NATIONAL DE RECHERCHE EN INFORMATIQUE ET EN AUTOMATIQUE
INRIA
centre de recherche GRENOBLE - RHÔNE-ALPES

Passivity-based tracking control of multiconstraint complementarity Lagrangian systems

Irinel–Constantin Morărescu*†, Bernard Brogliato‡†

Thème NUM — Systèmes numériques
Équipes-Projets BIPOP

Rapport de recherche n° 6483 — Mars 2008 — 32 pages

Abstract: In this study one considers the tracking control problem of a class of nonsmooth fully actuated Lagrangian systems subject to frictionless unilateral constraints. A passivity-based switching controller that guarantees some stability properties of the closed-loop system is designed. A particular attention is paid to transition (impacting) and detachment phases of motion. This paper extends previous works on the topic as it considers multiconstraint n-degree-of-freedom systems.

Key-words: Lagrangian systems, Complementarity problem, Impacts, Stability, Tracking control, Passivity-based control, Nonsmooth systems.

* constantin.morarescu@inrialpes.fr
† INRIA, Inovallée, 655 avenue de l'Europe, 38330, Montbonnot, France.
‡ bernard.brogliato@inrialpes.fr

Centre de recherche INRIA Grenoble – Rhône-Alpes
655, avenue de l'Europe, 38334 Montbonnot Saint Ismier
Téléphone : +33 4 76 61 52 00 — Télécopie +33 4 76 61 52 52

Commande passive pour la poursuite de trajectoires dans les systèmes Lagrangiens non-réguliers multi-contraintes

Résumé : Dans cette étude, on considère le problème de la commande pour assurer la poursuite des trajectoires pour une classe de systèmes Lagrangiens non-réguliers soumis à des contraintes unilatérales sans frottement. Une commande basée sur la passivité garantit certaines propriétés de stabilité pour le système en boucle fermée. Une attention particulière est accordée aux phases de transition avec impacts et aux phases de détachement. Ce travail étend précédents travaux sur le sujet car on considère des systèmes avec plusieurs contraintes et n- degré de liberté.

Mots-clés : Systèmes Lagrangiens, Probleme de complémentarité, Impacts, Stabilité, Poursuite des trajectoires, Commande basé sur la passivité, Systèmes non-réguliers

Contents

1 Introduction **3**

2 Basic concepts **6**
2.1 Typical task 6
2.2 Stability analysis criteria 7

3 Controller design **10**

4 Tracking control framework **11**
4.1 Design of the desired trajectories 12
4.2 Design of $q_d^*(\cdot)$ and $q_d(\cdot)$ on the phases $I_k^{J_k}$ 13

5 Design of the desired contact force during constraint phases **15**

6 Strategy for take-off at the end of constraint phases Ω_{2k+1}^J **16**

7 Closed-loop stability analysis **18**

8 Illustrative example **23**
8.1 Dynamics Equation based on Lagrangian formulation 23
8.2 Some remarks concerning the simulation scheme 24
8.3 The influence of the time-step on the closed-loop dynamics 26
8.4 The influence of controller parameters on the closed-loop dynamics . 27

9 Conclusions **29**

10 Appendix **30**
10.1 Computation details for inequality (29) 30

1 Introduction

The tracking control problem under consideration was studied in [7] mainly in the 1-dof (degree-of-freedom) case and in [4] in the n-dof case. Both of these paper consider systems with only one unilateral frictionless constraint. Here we not only consider the multiconstraint case but the results in Section 7 relax some very hard to verify condition imposed in [4]. We note that in the case of a single nonsmooth impact the exponential stability and bounded-input bounded state (BIBS) stability was studied in [17] using a state feedback control law. A study for a multiple degrees-of-freedom linear systems subject to nonsmooth impacts can be found in [18]. That approach proposes a proportional-derivative control law in order to study BIBS stability via Lyapunov techniques. Another approach for the tracking control of nonsmooth mechanical systems (so-called billiards) can be found in [10, 16].

This paper focuses on the problem of tracking control of complementarity Lagrangian systems [19] subject to frictionless unilateral constraints whose dynamics may be expressed as:

$$\begin{cases} M(X)\ddot{X} + C(X,\dot{X})\dot{X} + G(X) = U + \nabla F(X)\lambda_X \\ 0 \leq \lambda_X \perp F(X) \geq 0, \\ \text{Collision rule} \end{cases} \tag{1}$$

where $X(t) \in \mathbb{R}^n$ is the vector of generalized coordinates, $M(X) = M^T(X) \in \mathbb{R}^{n\times n}$ is the positive definite inertia matrix, $F(X) \in \mathbb{R}^m$ represents the distance to the constraints, $C(X, \dot{X})$ is the matrix containing Coriolis and centripetal forces, $G(X)$ contains conservative forces, $\lambda_X \in \mathbb{R}^m$ is the vector of the Lagrangian multipliers associated to the constraints and $U \in \mathbb{R}^n$ is the vector of generalized torque inputs. For the sake of completeness we precise that ∇ denotes the Euclidean gradient $\nabla F(X) = (\nabla F_1(X), \ldots, \nabla F_m(X)) \in \mathbb{R}^{n\times m}$ where $\nabla F_i(X) \in \mathbb{R}^n$ represents the vector of partial derivatives of $F_i(\cdot)$ w.r.t. the components of X. We assume that the functions $F_i(\cdot)$ are continuously differentiable and that $\nabla F_i(X) \neq 0$ for all X with $F_i(X) = 0$. It is worth to precise here that for a given function $f(\cdot)$ its derivative w.r.t. the time t will be denoted by $\dot{f}(\cdot)$. For any function $f(\cdot)$ the limit to the right at the instant t will be denoted by $f(t^+)$ and the limit to the left will be denoted by $f(t^-)$. A simple jump of the function $f(\cdot)$ at the moment $t = t_\ell$ is denoted $\sigma_f(t_\ell) = f(t_\ell^+) - f(t_\ell^-)$.

Definition 1 *A Linear Complementarity Problem (LCP) is a system given by:*

$$\begin{cases} \lambda \geq 0 \\ A\lambda + b \geq 0 \\ \lambda^T(A\lambda + b) = 0 \end{cases} \tag{2}$$

which is compactly re-written as

$$0 \leq \lambda \perp A\lambda + b \geq 0 \tag{3}$$

Such an LCP has a unique solution for all b if and only if A is a P-matrix [9].

The admissible domain associated to the system (1) is the closed set Φ where the system can evolve and it is described as follows:

$$\Phi = \{X \mid F(X) \geq 0\} = \bigcap_{1\leq i\leq m} \Phi_i,$$

where $\Phi_i = \{X \mid F_i(X) \geq 0\}$ considering that a vector is non-negative if and only if all its components are non-negative. In order to have a well-posed problem with a physical meaning we consider that Φ contains at least a closed ball of positive radius.

Definition 2 *A singularity of the boundary $\partial\Phi$ of Φ is the intersection of two or more codimension one surfaces $\Sigma_i = \{X \mid F_i(X) = 0\}$.*

The presence of $\partial\Phi$ may induce some impacts that must be included in the dynamics of the system. It is obvious that $m > 1$ allows both simple impacts (when one constraint is involved) and multiple impacts (when singularities or surfaces of codimension larger than 1 are involved). In order to simplify the presentation we introduce the following notion of p_ϵ-impact.

Definition 3 *Let $\epsilon \geq 0$ be a fixed real number. We say that a p_ϵ-impact occurs at the instant t if*

$$||F_I(X(t))|| \leq \epsilon, \quad \prod_{i\in I} F_i(X(t)) = 0$$

where $I \subset 1, \ldots, m$, $card(I) = p$.

If $\epsilon = 0$ the p surfaces Σ_i, $i \in I$ are stroked simultaneously. When $\epsilon > 0$ the system collides $\partial\Phi$ in a neighborhood of the intersection $\bigcap_{i\in I} \Sigma_i$.

Definition 4 *[19, 22] The tangent cone to* $\Phi = \{X \mid F_i(X) \geq 0, \forall i = 1, \ldots, n\}$ *at* $q \in \mathbb{R}^n$ *is defined as:*

$$T_\Phi(q) = \{z \in \mathbb{R}^n \mid z^T \nabla F_i(q) \geq 0, \forall i = J(q)\}$$

where $J(q) \triangleq \{i \in \{1, \ldots, n\} \mid F_i(q) \leq 0\}$*. When* $q \in \Phi \setminus \partial\Phi$ *one has* $J(q) = \emptyset$ *and* $T_\Phi(q) = \mathbb{R}^n$*.*
The normal cone to Φ *at* q *is defined as the polar cone to* $T_\Phi(\cdot)$*:*

$$N_\Phi(q) = \{y \in \mathbb{R}^n \mid \forall z \in T_\Phi(q), y^T z \leq 0\}$$

The collision (or restitution) rule in (1), is a relation between the post-impact velocity and the pre-impact velocity. Among the various models of collision rules, Moreau's rule is an extension of Newton's law which is energetically consistent [12] and is numerically tractable [1]. For these reasons throughout this paper the collision rule will be defined by Moreau's relation [19]:

$$\dot{X}(t_\ell^+) = (1+e) \underset{z \in T_\Phi(X(t_\ell))}{\arg\min} \frac{1}{2}[z - \dot{X}(t_\ell^-)]^T \times M(X(t_\ell))[z - \dot{X}(t_\ell^-)] - e\dot{X}(t_\ell^-) \quad (4)$$

where $\dot{X}(t_\ell^+)$ is the post-impact velocity, $\dot{X}(t_\ell^-)$ is the pre-impact velocity and $e \in [0, 1]$ is the restitution coefficient. Denoting by T the kinetic energy of the system, we can compute the kinetic energy loss at the impact t_ℓ as [14]:

$$T_L(t_\ell) = -\frac{1-e}{2(1+e)}\Big[\dot{X}(t_\ell^+) - \dot{X}(t_\ell^-)]^T M(X(t_\ell)) \times [\dot{X}(t_\ell^+) - \dot{X}(t_\ell^-)\Big] \leq 0 \quad (5)$$

The collision rule can be rewritten considering the vector of generalized velocities as an element of the tangent space to the configuration space of the system, equipped with the kinetic energy metric. Doing so (see [5] §6.2), the discontinuous velocity components $\dot{X}_{norm}$ and the continuous ones $\dot{X}_{tang}$ are identified. Precisely, $\begin{pmatrix} \dot{X}_{norm} \\ \dot{X}_{tang} \end{pmatrix} = \mathcal{M}\dot{X}$, $\mathcal{M} = \begin{pmatrix} \mathbf{n}^T \\ \mathbf{t}^T \end{pmatrix} M(X)$ where $\mathbf{n} \in \mathbb{R}^m$ represents the m unitary normal vectors $\mathbf{n}_i = \frac{M^{-1}(X)\nabla F_i(X)}{\sqrt{\nabla F_i(X)^T M^{-1}(X) \nabla F_i(X)}}$, $i = 1, \ldots, m$ and $\mathbf{t}$ represents $n - m$ mutually independent unitary vectors $\mathbf{t}_i$ such that $\mathbf{t}_i^T M(X)\mathbf{n}_j = 0, \forall i, j$. In this case the collision rule (4) at the impact time t_ℓ becomes the generalized Newton's rule $\begin{pmatrix} \dot{X}_{norm}(t_\ell^+) \\ \dot{X}_{tang}(t_\ell^+) \end{pmatrix} = -\eta \begin{pmatrix} \dot{X}_{norm}(t_\ell^-) \\ \dot{X}_{tang}(t_\ell^-) \end{pmatrix}$, $\eta = diag(e_1, \ldots, e_m, 0, \ldots, 0)$ where e_i is the restitution coefficient w.r.t. the surface Σ_i. For the sake of simplicity we consider in this paper that all the restitution coefficients are equal, i.e. $e_1 = \ldots = e_m \triangleq e$.

Remark 1 *1) If* $X \in \Sigma_1 \bigcap \Sigma_2$ *and the angle* $\angle(\Sigma_1, \Sigma_2) \leq \pi$ *then in the neighborhood of* X *one has* $\Phi \simeq T_\Phi(X)$*.*

2) The case $e = 0$ *is called a plastic impact and the case* $e = 1$ *is called an elastic impact. In the first case the normal component of the velocity becomes zero and in the second case the normal component of the velocity changes only its direction and preserves its magnitude. As we can easily see from (5) in the second case there is no loss of kinetic energy at the impact moment.*

3) *One recalls that we deal with frictionless unilateral constraints. Some frictional contact laws that fit within the nonsmooth mechanic framework (1) can be found in [13].*

The structure of the paper is as follows: in Section 2 one presents some basic concepts and prerequisites necessary for the further developments. Section 3 is devoted to the controller design. In Section 4 one defines the desired (or "exogenous") trajectories entering the dynamics. The desired contact-force that must occur on the phases where the motion is constrained, is explicitly defined in Section 5. Section 6 focuses on the strategy for take-off at the end of the constraint phases. The main results related to the closed-loop stability analysis are presented in Section 7. One example and concluding remarks end the paper.

The following standard notations will be adopted: $||\cdot||$ is the Euclidean norm, $b_p \in \mathbb{R}^p$ and $b_{n-p} \in \mathbb{R}^{n-p}$ are the vectors formed with the first p and the last $n-p$ components of $b \in \mathbb{R}^n$, respectively. $N_\Phi(X_p = 0)$ is the normal cone $N_\Phi(X)$ to Φ at X [19, 22] when X satisfies $X_p = 0$, $\lambda_{min}(\cdot)$ and $\lambda_{max}(\cdot)$ represent the smallest and the largest eigenvalues, respectively.

2 Basic concepts

2.1 Typical task

In the case $m = 1$ (only one unilateral constraint) the time axis can be split into intervals Ω_k and I_k corresponding to specific phases of motion [7]. Precisely, Ω_{2k} corresponds to free-motion phases ($F(X) > 0$) and Ω_{2k+1} corresponds to constrained-motion phases ($F(X) = 0$). Between free and constrained phases the dynamical system always passes into a transition phase I_k containing some impacts. Since the dynamics of the system does not change during the transition between constrained and free-motion phases, in the time domain one gets the following typical task representation:

$$\mathbb{R}^+ = \Omega_0 \cup I_0 \cup \Omega_1 \cup \Omega_2 \cup I_1 \cup \ldots \cup \Omega_{2k} \cup I_k \cup \Omega_{2k+1} \cup \ldots \tag{6}$$

In the case $m \geq 2$ (multiple constraints) things complicate since the number of typical phases increases due to the singularities that must be taken into account. Explicitly, the constrained-motion phases need to be decomposed in sub-phases where some specific constraints are active. Between two such sub-phases a transition phase occurs when the number of active constraints increases. Nevertheless, a typical task can be represented in the time domain as:

$$\begin{gathered}\mathbb{R}^+ = \bigcup_{k\geq 0}\left(\Omega_{2k}^{J_k} \cup I_k^{J_k} \cup \left(\bigcup_{i=1}^{m_k} \Omega_{2k+1}^{J_{k,i}}\right)\right) \\ J_k \subset J_{k,1};\ J_{k+1} \subset J_{k,m_k} \subset J_{k,m_k-1} \subset \ldots J_{k,1}\end{gathered} \tag{7}$$

where the superscript J_k represents the set of active constraints ($J_k = \{i \in \{1,\ldots,m\} \mid F_i(X) = 0\}$) during the corresponding motion phase, and $I_k^{J_k}$ denotes the transient between two Ω_k phases when the number of active constraints increases. When the number of active constraints decreases there is no impact, thus no other transition phases are needed. We note that $J_k = \emptyset$ corresponds to free-motion.

For the sake of simplicity and without any loss of generality we replace $\bigcup_{i=1}^{m_k} \Omega_{2k+1}^{J_{k,i}}$ by $\Omega_{2k+1}^{J'_k}$ where $J_k \subset J'_k$ and $J_{k+1} \subset J'_k$. Therefore the typical task simplifies as:

$$\begin{aligned} \mathbb{R}^+ = \bigcup_{k\geq 0} \left(\Omega_{2k}^{J_k} \cup I_k^{J_k} \cup \Omega_{2k+1}^{J'_k}\right) \\ J_k \subset J'_k, \quad J_{k+1} \subset J'_k \end{aligned} \tag{8}$$

Since the tracking control problem involves no difficulty during the Ω_k phases, *the central issue is the study of the passages between them (the design of transition phases I_k and detachment conditions), and the stability of the trajectories evolving along (8)* (i.e. an infinity of cycles). Throughout the paper, the sequence $\Omega_{2k}^{J_k} \cup I_k^{J_k} \cup \Omega_{2k+1}^{J'_k}$ will be referred to as the cycle k of the system's evolution. For robustness reasons during transition phases I_k we impose a closed-loop dynamics (containing impacts) that mimics somehow the bouncing-ball dynamics (see e.g. [5]).

2.2 Stability analysis criteria

The system (1) is a complex nonsmooth and nonlinear dynamical system which involves continuous and discrete time phases. A stability framework for this type of systems has been proposed in [7] and extended in [4]. This is an extension of the Lyapunov second method adapted to closed-loop mechanical systems with unilateral constraints. Since we use this criterion in the following tracking control strategy it is worth to clarify the framework and to introduce some definitions.
Let us introduce the trajectories playing a role in the dynamics and the design of the controller:

- $X^{nc}(\cdot)$ denotes the desired trajectory of the unconstrained system (i.e. the trajectory that the system should track if there were no constraints). We suppose that $F(X^{nc}(t)) < 0$ for some t, otherwise the problem reduces to the tracking control of a system with no constraints.
- $X_d^*(\cdot)$ denotes the signal entering the control input and playing the role of the desired trajectory during some parts of the motion.
- $X_d(\cdot)$ represents the signal entering the Lyapunov function. This signal is set on the boundary $\partial\Phi$ after the first impact of each cycle.

These signals may coincide on some time intervals as we shall see later. In order to clarify the differences and the usefulness of these signals we present a simple example concerning a one-degree of freedom model.

Example 1 *Let us consider the following one degree-of-freedom dynamical system:*

$$\begin{cases} (\ddot{X} - \ddot{X}_d^*) + \gamma_2(\dot{X} - \dot{X}_d^*) + \gamma_1(X - X_d^*) = \lambda \\ 0 \leq X \perp \lambda \geq 0 \\ \dot{X}(t_k^+) = -e_n \dot{X}(t_k^-) \end{cases} \tag{9}$$

where $X_d^*(\cdot)$ is a twice differentiable signal and γ_1, γ_2 are two gains. The real number λ represents the Lagrange multiplier associated to the constraint $X \geq 0$.

The system (9) represents the dynamics of a unitary mass lying in the right half plane ($X \geq 0$) and moving on the Ox axis (see figure 1). Thus, the system dynamics is

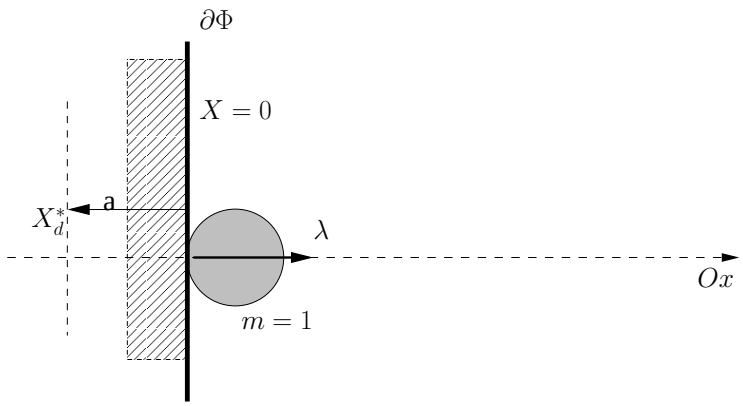

Figure 1: One degree of freedom: unitary mass dynamics

expressed by $\ddot{X} = U + \lambda$ *with the control law* $U = \ddot{X}_d^* - \gamma_2(\dot{X} - \dot{X}_d^*) - \gamma_1(X - X_d^*)$. *One considers that the Lyapunov function* $V(X, \dot{X}, t)$ *of the closed-loop system is given by a quadratic function of the tracking error.*

In order to stabilize the system on the constraint surface $\partial\Phi$ *there are two solutions.*

[1st solution] *Setting* $X_d^*(t) = 0$, $\dot{X}_d^*(t) = 0$ *and* $\ddot{X}_d^*(t) = 0$ *at the time* t *of contact with* $\partial\Phi$. *Therefore when the system reaches its equilibrium point on* $\partial\Phi$ *one obtains the contact force* $\lambda = 0$. *It is noteworthy that, since we are interested to study a dynamics containing a constraint movement phase, we need a non-zero contact force when the system is stabilized on* $\partial\Phi$. *Therefore this type of solution is not convenient for the study developed in this work. Moreover the stabilization on* $\partial\Phi$ *with a non zero tracking error on* $[t - \epsilon, t]$ *is not obvious, especially in higher dimensions, so that the conditions for a perfect tangential approach are never met in practice.*

[2nd solution] *Setting* $X_d^*(t) = -a$, $a > 0$, $\dot{X}_d^*(t) = 0$ *and* $\ddot{X}_d^*(t) = 0$ *on some interval of time when approaching* $\partial\Phi$. *Since the tracking error* $\bar{X} = X - X_d^* = -X_d^*$ *at the equilibrium point we cannot use* $\bar{X}$ *in the definition of the Lyapunov function. Obviously the system reaches the desired position when* $X = 0$. *Thus we shall use the signal* $X_d(t) = 0$ *in order to express the desired trajectory in the Lyapunov function and the corresponding tracking error will be given by* $\tilde{X} = X - X_d$. *Concluding, when the equilibrium point is reached one obtains* $\tilde{X} = 0$, $\bar{X} = -a$, $V(t, \tilde{X} = 0) = 0$ *and the corresponding contact force* $\lambda = -\gamma_1 X_d^* = \gamma_1 a > 0$.

Next, let us define Ω as the complement of $I = \bigcup_{k \geq 0} I_k^{J_k}$ and assume that the Lebesgue measure of Ω, denoted $\lambda[\Omega]$, equals infinity. Consider $x(\cdot)$ the state of the closed-loop system in (1) with some feedback controller $U(X, \dot{X}, X_d^*, \dot{X}_d^*, \ddot{X}_d^*)$.

Definition 5 (Weakly Stable System [4]) *The closed loop system is called weakly stable if for each* $\epsilon > 0$ *there exists* $\delta(\epsilon) > 0$ *such that* $||x(0)|| \leq \delta(\epsilon) \Rightarrow ||x(t)|| \leq \epsilon$ *for all* $t \geq 0$, $t \in \Omega$. *The system is asymptotically weakly stable if it is weakly stable and* $\lim_{t \in \Omega,\, t \to \infty} x(t) = 0$. *Finally, the practical weak stability holds if there exists* $0 < R < +\infty$ *and* $t^* < +\infty$ *such that* $||x(t)|| < R$ *for all* $t > t^*$, $t \in \Omega$.

Consider $I_k^{J_k} \triangleq [\tau_0^k, t_f^k]$ and $V(\cdot)$ such that there exists strictly increasing functions $\alpha(\cdot)$ and $\beta(\cdot)$ satisfying the conditions: $\alpha(0) = 0$, $\beta(0) = 0$ and $\alpha(||x||) \leq V(x, t) \leq$

$\beta(||x||)$.
In the sequel, we consider that for each cycle k the sequence of impact instants t_ℓ^k has an accumulation point t_∞^k. We note that a finite accumulation period (i.e. $t_\infty^k < +\infty$) implies that $e < 1$ (in [3] it is shown that $e = 1$ implies that $t_\infty^k = +\infty$).

The following criterion is inspired from [4], and will be used for studying the stability of system (1).

Proposition 1 (Weak Stability) *Assume that the task admits the representation (8) and that*

a) $\lambda[I_k^{J_k}] < +\infty, \quad \forall k \in \mathbb{N}$,

b) *outside the impact accumulation phases* $[t_0^k, t_\infty^k]$ *one has* $\dot{V}(x(t), t) \leq -\gamma V(x(t), t)$ *for some constant* $\gamma > 0$,

c) $\sum_{\ell \geq 0} \left[V(t_{\ell+1}^{k-}) - V(t_\ell^{k+})\right] \leq K_1 V^{p_1}(\tau_0^k), \quad \forall \ell \geq 0$ *for some* $p_1 \geq 0,\ K_1 \geq 0$,

d) *the system is initialized on* Ω_0 *such that* $V(\tau_0^0) \leq 1$,

e) $\sum_{\ell \geq 0} \sigma_V(t_\ell^k) \leq K_2 V^{p_2}(\tau_0^k) + \xi$ *for some* $p_2 \geq 0,\ K_2 \geq 0$ *and* $\xi \geq 0$.

If $p = \min\{p_1, p_2\} < 1$ *then* $V(\tau_0^k) \leq \delta(\gamma, \xi)$, *where* $\delta(\gamma, \xi)$ *is a function that can be made arbitrarily small by increasing the value of* γ. *The system is practically weakly stable with* $R = \alpha^{-1}(\delta(\gamma, \xi))$.

Proof: From assumption (b) one has

$$V(t_f^k) \leq V(t_\infty^k) e^{-\gamma(t_f^k - t_\infty^k)}$$

It is clear that condition (c) combined with (e) leads to

$$V(t_\infty^k) \leq V(\tau_0^k) + K_1 V^{p_1}(\tau_0^k) + K_2 V^{p_2}(\tau_0^k) + \xi$$

Considering $p < 1$, the assumption (d) guarantees that $\max\{V(\tau_0^k), V^{p_1}(\tau_0^k), V^{p_2}(\tau_0^k)\}$ $\leq V^p(\tau_0^k) \leq 1$ and we get

$$\begin{aligned} V(t_f^k) &\leq e^{-\gamma(t_f^k - t_\infty^k)} \left[1 + K_1 + K_2 + \xi\right] V^p(\tau_0^k) \\ &\leq e^{-\gamma(t_f^k - t_\infty^k)} \left[1 + K_1 + K_2 + \xi\right] \triangleq \delta(\gamma, \xi) \end{aligned}$$

From assumption (b) one has $V(\tau_0^{k+1}) \leq V(t_f^k)$ thus the first part of the statement holds. The term $\delta(\gamma, \xi)$ can be made as small as desired increasing either γ or the length of the interval $[t_\infty^k, t_f^k]$. The proof is completed by the relation $\alpha(||x||) \leq V(x, t),\ \forall x,\ t$

Remark 2 *Since the Lyapunov function is exponentially decreasing on the* Ω_k *phases, assumption (d) in Proposition 1 means that the system is initialized on* Ω_0 *sufficiently far from the moment when the trajectory* $X^{nc}(\cdot)$ *leaves the admissible domain.*

Precisely, the weak stability is characterized by an "almost decreasing" Lyapunov function $V(x(\cdot).\cdot)$ as illustrated in Figure 2.

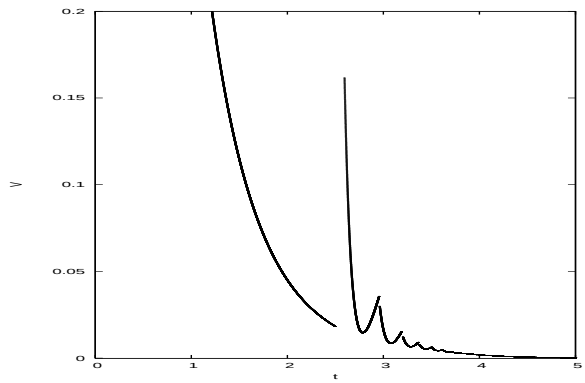

Figure 2: Typical evolution of the Lyapunov function during one cycle of a weakly stable system.

Remark 3 *It is worth to point out the local character of the stability criterion proposed by Proposition 1. This character is firstly given by condition d) of the statement and secondly by the synchronization constraints of the control law and the motion phase of the system (see (10) and (8) below).*

The practical stability is very useful because attaining asymptotic stability is not an easy task for the unilaterally constrained systems described by (1) especially when $n \geq 2$ and $M(q)$ is not a diagonal matrix (i.e. there are inertial couplings, which is the general case).

3 Controller design

In order to overcome some difficulties that can appear in the controller definition, the dynamical equations (1) will be expressed in the generalized coordinates introduced by McClamroch & Wang [15]. We suppose that the generalized coordinates transformation holds globally in Φ, which may obviously not be the case in general. However, the study of the singularities that might be generated by the coordinates transformation is out of the scope of this paper. Let us consider $D = [I_m \vdots O] \in \mathbb{R}^{m\times n}$, $I_m \in \mathbb{R}^{m\times m}$ the identity matrix. The new coordinates will be $q = Q(X) \in \mathbb{R}^n$, with $q = \begin{bmatrix} q_1 \\ q_2 \end{bmatrix}$, $q_1 = \begin{bmatrix} q_1^1 \\ \vdots \\ q_1^m \end{bmatrix}$ such that $\Phi = \{q \mid Dq \geq 0\}$[1]. The tangent cone $T_\Phi(q_1 = 0) = \{v \mid Dv \geq 0\}$ is the space of admissible velocities on the boundary of Φ.

The controller used here consists of different low-level control laws for each phase of the system. More precisely, the switching controller can be expressed as

$$T(q)U = \begin{cases} U_{nc} & \text{for } t \in \Omega_{2k}^{\emptyset} \\ U_t^J & \text{for } t \in I_k^J \\ U_c^J & \text{for } t \in \Omega_k^J \end{cases} \tag{10}$$

[1]In particular it is implicitly assumed that the function $F_i(\cdot)$ in (1) are linearly independent

where $T(q) = \begin{pmatrix} T_1(q) \\ T_2(q) \end{pmatrix} \in \mathbb{R}^{n\times n}$ is full-rank under some basic assumptions (see [15]). The dynamics becomes:

$$\begin{cases} M_{11}(q)\ddot{q}_1 + M_{12}(q)\ddot{q}_2 + C_1(q,\dot{q})\dot{q} + g_1(q) &= T_1(q)U + \lambda \\ M_{21}(q)\ddot{q}_1 + M_{22}(q)\ddot{q}_2 + C_2(q,\dot{q})\dot{q} + g_2(q) &= T_2(q)U \\ q_1^i \geq 0,\ q_1^i\lambda_i = 0,\ \lambda_i \geq 0,\ 1 \leq i \leq m \\ \text{Collision rule} \end{cases} \tag{11}$$

where the set of complementary relations can be written more compactly as $0 \leq \lambda \perp Dq \geq 0$.

In the sequel U_{nc} coincides with the fixed-parameter controller proposed in [20, 21] and the closed-loop stability analysis of the system is based on Proposition 1. First, let us introduce some notations: $\tilde{q} = q - q_d$, $\bar{q} = q - q_d^*$, $s = \dot{\tilde{q}} + \gamma_2\tilde{q}$, $\bar{s} = \dot{\bar{q}} + \gamma_2\bar{q}$, $\dot{q}_e = \dot{q}_d - \gamma_2\tilde{q}$ where $\gamma_2 > 0$ is a scalar gain and q_d, q_d^* represent the desired trajectories defined in the previous section. Using the above notations the controller is given by

$$T(q)U \triangleq \begin{cases} U_{nc} &= M(q)\ddot{q}_e + C(q,\dot{q})\dot{q}_e + G(q) - \gamma_1 s \\ U_t^J &= U_{nc}^J,\ t \leq t_0^k \\ U_t^J &= M(q)\ddot{q}_e + C(q,\dot{q})\dot{q}_e + G(q) - \gamma_1\bar{s},,\ t > t_0^k \\ U_c^J &= U_{nc} - P_d + K_f(P_q - P_d) \end{cases} \tag{12}$$

where $\gamma_1 > 0$ is a scalar gain, $K_f > 0$, $P_q = D^T\lambda$ and $P_d = D^T\lambda_d$ is the desired contact force during persistently constrained motion. It is clear that during Ω_k^J not all the constraints are active and, therefore, some components of λ and λ_d are zero.

In order to prove the stability of the closed-loop system (11) - (12) we will use the following positive definite function:

$$V(t,s,\tilde{q}) = \frac{1}{2}s^T M(q)s + \gamma_1\gamma_2\tilde{q}^T\tilde{q} \tag{13}$$

4 Tracking control framework

In this paper we treat the tracking control problem for the closed-loop dynamical system (10)–(12) with the complete desired path a priori taking into account the complementarity conditions and the impacts. In order to define the desired trajectory let us consider the motion of a virtual and unconstrained particle perfectly following a trajectory (represented by $X^{nc}(\cdot)$ on Figure 3) with an orbit that leaves the admissible domain for a given period. Therefore, the orbit of the virtual particle can be split into two parts, one of them belonging to the admissible domain (inner part) and the other one outside the admissible domain (outer part). In the sequel we deal with the tracking control strategy when the desired trajectory is constructed such that:

(i) when no activated constraints, it coincides with the trajectory of the virtual particle (the desired path and velocity are defined by the path and velocity of the virtual particle, respectively),

(ii) when $p \leq m$ constraints are active, its orbit coincides with the projection of the outer part of the virtual particle's orbit on the surface of codimension p defined by the activated constraints (X_d between A'' and C in Figure 3),

(iii) the desired detachment moment and the moment when the virtual particle re-enters the admissible domain (with respect to $p \leq m$ constraints) are synchronized.

Therefore we have not only to track a desired path but also to impose a desired velocity allowing the motion synchronization on the admissible domain.

The main difficulties here consist of:

- stabilizing the system on $\partial\Phi$ during the transition phases $I_k^{J_k}$ and incorporating the velocity jumps in the overall stability analysis;
- deactivating some constraints at the moment when the unconstrained trajectory re-enters the admissible domain with respect to them;
- maintaining a constraint movement between the moment when the system was stabilized on $\partial\Phi$ and the detachment moment.

Remark 4 *The problem can be relaxed considering that we want to track only a desired path like $X^{nc}(\cdot)$ (without imposing a desired velocity on the inner part of the desired trajectory and/or a given period to complete a cycle). In this way the synchronization problem (iii) disappears and we can assume there exists a twice differentiable desired trajectory outside $[t_0^k, t_f^k]$ that assures the detachment when the force control is dropped. In other words, in this case we have to design the desired trajectory only during $I_k^{J_k}$ phases.*

4.1 Design of the desired trajectories

Throughout the paper we consider $I_k^{J_k} = [\tau_0^k, t_f^k]$, where τ_0^k is chosen by the designer as the start of the transition phase $I_k^{J_k}$ and t_f^k is the end of $I_k^{J_k}$. We note that all superscripts $(\cdot)^k$ will refer to the cycle k of the system motion. We also use the following notations:

- t_0^k is the first impact during the cycle k,
- t_∞^k is the accumulation point of the sequence $\{t_\ell^k\}_{\ell\geq 0}$ of the impact instants during the cycle k ($t_f^k \geq t_\infty^k$),
- τ_1^k will be explicitly defined later and represents the instant when the desired signal X_d^* reaches a given value chosen by the designer in order to impose a closed-loop dynamics with impacts during transition phases,
- t_d^k is the desired detachment instant, therefore the phases $\Omega_{2k+1}^{J'_k}$ can be expressed as $[t_f^k, t_d^k]$.

It is noteworthy that t_0^k, t_∞^k, t_d^k are state-dependent whereas τ_1^k and τ_0^k are exogenous and imposed by the designer. To better understand the definition of these specific instants, in the Figure 3 we simplify the system's motion as follows:

- during transition phases we take into account only the constraints that must be activated $J'_k \setminus J_k$.
- at the end of Ω_{2k+1} phases we take into account only the constraints that must be deactivated $J'_k \setminus J_{k+1}$.

The points A, A', A'' and C in Figure 3 correspond to the moments τ_0^k, t_0^k, t_f^k and t_d^k respectively. We have seen that the choice of τ_0^k plays an important role in the stability criterion given by Proposition 1. On the other hand in Figure 3 we see that

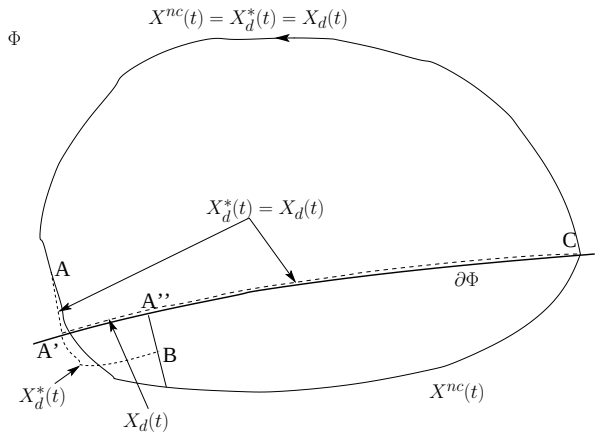

Figure 3: The closed-loop desired trajectory and control signals

starting from A the desired trajectory $X_d(\cdot) = X_d^*(\cdot)$ is deformed compared to $X^{nc}(\cdot)$. In order to reduce this deformation τ_0^k and implicitly the point A must be close to $\partial\Phi$ (see also Figure 6). Further details on the choice of τ_0^k will be given later. Taking into account just the constraints $J_k' \setminus J_{k+1}$ we can identify t_d^k with the moment when $X_d(\cdot)$ and $X^{nc}(\cdot)$ rejoin at C.

4.2 Design of $q_d^*(\cdot)$ and $q_d(\cdot)$ on the phases $I_k^{J_k}$

During the transition phases the system must be stabilized on $\partial\Phi$. Obviously, this does not mean that all the constraints have to be activated (i.e. $q_1^i(t) = 0$, $\forall i = 1, \ldots, m$). Let us consider that only the first p constraints (eventually reordering the coordinates) define the border of Φ where the system must be stabilized. On $[\tau_0^k, t_0^k)$ we define $q_d^*(\cdot)$ as a twice differentiable signal such that $q_d^*(\cdot)$ approaches a given point in the normal cone $N_\Phi(q_p = 0)$ on $[\tau_0^k, \tau_1^k]$. Precisely, we define $q_d^*(\cdot)$ such as:

- during a small period $\delta > 0$ chosen by the designer the desired velocity becomes zero preserving the twice differentiability of $q_d^*(\cdot)$. For instance we can use the following definition:

$$q_d^*(t) = q^{nc}\left(\tau_0^k + \frac{(t-\tau_0^k-\delta)^2(t-\tau_0^k)}{\delta^2}\right), t \in [\tau_0^k, \tau_0^k + \delta]$$

  which means $q_d^*(\tau_0^k + \delta) = q_d^*(\tau_0^k) = q^{nc}(\tau_0^k)$, $\quad \dot{q}_d^*(\tau_0^k + \delta) = 0$ and $\dot{q}_d^*(\tau_0^k) = \dot{q}^{nc}(\tau_0^k)$

- choosing $\varphi > 0$ and denoting $t' = \frac{t-(\tau_0^k+\delta)}{\tau_1^k-(\tau_0^k+\delta)}$, the components $\left(q_d^i\right)^*$, $i = 1, \ldots, p$ of $\left(q_d^*\right)_p$ are defined as:

$$\left(q_d^i\right)^*(t) = \begin{cases} a_3(t')^3 + a_2(t')^2 + a_0, & t \in [\tau_0^k + \delta, \min\{\tau_1^k; t_0^k\}] \\ -\varphi V^{1/3}(\tau_0^k), & t \in (\min\{\tau_1^k; t_0^k\}, t_f^k] \end{cases} \tag{14}$$

  where $V(\cdot)$ is defined in (13) and with the coefficients given by:

$$\begin{array}{rcl} a_3 & = & 2[\left(q^i\right)^{nc}(\tau_0^k) + \varphi V^{1/3}(\tau_0^k)] \\ a_2 & = & -3[\left(q^i\right)^{nc}(\tau_0^k) + \varphi V^{1/3}(\tau_0^k)] \\ a_0 & = & \left(q^i\right)^{nc}(\tau_0^k) \end{array} \tag{15}$$

- all the other components of $q_d^*(\cdot)$ are frozen:

$$(q_d^*)_{n-p}(t) = q_{n-p}^{nc}(\tau_0^k), \quad t \in (\tau_0^k + \delta, t_f^k] \tag{16}$$

The rationale behind the choice of $q_d^*(\cdot)$ is on one hand to assure a robust stabilization on $\partial\Phi$, mimicking the bouncing-ball dynamics; on the other hand to enable one to compute suitable upper-bounds that will help using Proposition 1 (hence $V^{1/3}(\cdot)$ terms in (14) with $V(\cdot)$ in (13)).

Remark 5 *1) Straightforward computations show that $q_d^*(\cdot)$ satisfies the following relations.*

$$\left(q_d^i\right)^*(\tau_1^k) = -\varphi V^{1/3}(\tau_0^k), \quad \left(\dot{q}_d^i\right)^*(\tau_1^k) = 0,\ i = 1, \ldots, p$$

2) Two different situations are possible. The first is given by $t_0^k > \tau_1^k$ (see Figure 4) and we shall prove that in this situation all the jumps of the Lyapunov function in (13) are negative. The second situation was pointed out in [4] and is given by $t_0^k < \tau_1^k$. In this situation the first jump at t_0^k in the Lyapunov function is positive, therefore the system can be only weakly stable. It is noteworthy that $q_d^*(\cdot)$ will then have a jump at the time t_0^k since $(q_d^i)^*(t_0^{k+}) = -\varphi V^{1/3}(\tau_0^k)$, $\forall i = 1, \ldots, p$ (see (14)).

In order to limit the deformation of the desired trajectory $q_d^*(\cdot)$ w.r.t. the unconstrained trajectory $q^{nc}(\cdot)$ during the I_k phases (see Figure 3 and 4), we impose in the sequel

$$||q_p^{nc}(\tau_0^k)|| \leq \psi \tag{17}$$

where $\psi > 0$ is chosen by the designer. It is obvious that a smaller ψ leads to smaller deformation of the desired trajectory and to smaller deformation of the real trajectory as we shall see in Section 8. Nevertheless, due to the tracking error, ψ cannot be chosen zero. We also note that $||q_p^{nc}(\tau_0^k)|| \leq \psi$ is a practical way to choose τ_0^k.

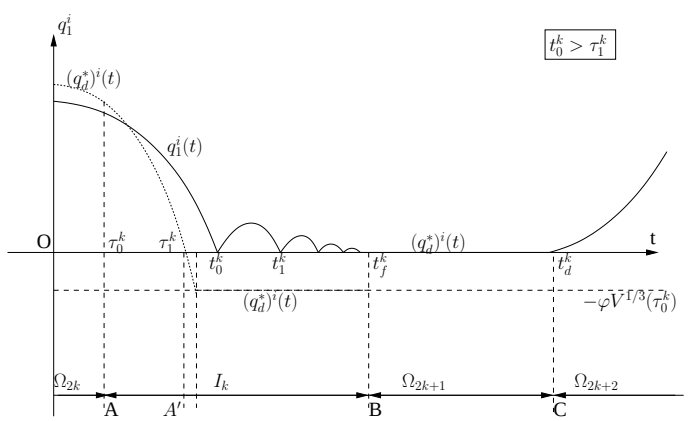

Figure 4: The design of q_{1d}^* on the transition phases I_k

During the transition phases I_k we define $(q_d)_{n-p}(t) = (q_d^*)_{n-p}(t)$. Assuming a finite accumulation period, the impact process can be considered in some way equivalent to a plastic impact. Therefore, $(q_d)_p(\cdot)$ and $(\dot{q}_d)_p(\cdot)$ are set to zero on the right of t_0^k.

5 Design of the desired contact force during constraint phases

For the sake of simplicity we consider the case of the constraint phase $\Omega_k^J,\ J \neq \emptyset$ with $J = \{1, \ldots, p\}$. Obviously a sufficiently large desired contact force P_d assures a constrained movement on Ω_k^J. Nevertheless at the end of the Ω_{2k+1}^J phases a detachment from some surfaces Σ_i has to take place. It is clear that a take-off implies not only a well-defined desired trajectory but also some small values of the corresponding contact force components. On the other hand, if the components of the desired contact force decrease too much a detachment can take place before the end of the Ω_k^J phases which can generate other impacts. Therefore we need a lower bound of the desired force which assures the contact during the Ω_k^J phases.
Dropping the time argument, the dynamics of the system on Ω_k^J can be written as

$$\left\{ \begin{array}{c} M(q)\ddot{q} + F(q,\dot{q}) = U_c + D_p^T \lambda_p \\ 0 \leq q_p \perp \lambda_p \geq 0 \end{array} \right. \tag{18}$$

where $F(q,\dot{q}) = C(q,\dot{q})\dot{q} + G(q)$ and $D_p = [I_p \vdots O] \in \mathbb{R}^{p \times n}$. On Ω_k^J the system is permanently constrained which implies $q_p(\cdot) = 0$ and $\dot{q}_p(\cdot) = 0$. In order to assure these conditions it is sufficient to have $\lambda_p > 0$.
In the following let us denote $M^{-1}(q) = \begin{pmatrix} [M^{-1}(q)]_{p,p} & [M^{-1}(q)]_{p,n-p} \\ [M^{-1}(q)]_{n-p,p} & [M^{-1}(q)]_{n-p,n-p} \end{pmatrix}$ and
$C(q,\dot{q}) = \begin{pmatrix} C(q,\dot{q})_{p,p} & C(q,\dot{q})_{p,n-p} \\ C(q,\dot{q})_{n-p,p} & C(q,\dot{q})_{n-p,n-p} \end{pmatrix}$ where the meaning of each component is obvious.

Proposition 2 *On Ω_k^J the constraint motion of the closed-loop system (18),(10),(12) is assured if the desired contact force is defined by*

$$\begin{array}{l} (\lambda_d)_p \triangleq \beta - \dfrac{\bar{M}_{p,p}(q)}{1+K_f} \left([M^{-1}(q)]_{p,p} C_{p,n-p}(q,\dot{q}) + \right. \\ \left. [M^{-1}(q)]_{p,n-p} C_{n-p,n-p}(q,\dot{q}) + \gamma_1 [M^{-1}(q)]_{p,n-p} \right) s_{n-p} \end{array} \tag{19}$$

where $\bar{M}_{p,p}(q) = \left([M^{-1}(q)]_{p,p}\right)^{-1} = \left(D_p M^{-1}(q) D_p^T\right)^{-1}$ is the inverse of the Delassus' matrix and $\beta \in \mathbb{R}^p,\ \beta > 0$.

Proof: First, we notice that the second relation in (18) implies on Ω_k^J (see [11])

$$0 \leq \ddot{q}_p \perp \lambda_p \geq 0 \Leftrightarrow 0 \leq D_p \ddot{q} \perp \lambda_p \geq 0. \tag{20}$$

From (18) and (12) one easily gets:

$$\ddot{q} = M^{-1}(q)\big[-F(q,\dot{q}) + U_{nc} + (1+K_f) D_p^T (\lambda - \lambda_d)_p \big]$$

Combining the last two equations we obtain the following LCP with unknown λ_p:

$$\begin{array}{c} 0 \leq D_p M^{-1}(q)\big[-F(q,\dot{q}) + U_{nc} - (1+K_f) D_p^T (\lambda_d)_p \big] \\ +(1+K_f) D_p M^{-1}(q) D_p^T \lambda_p \perp \lambda_p \geq 0 \end{array} \tag{21}$$

Since $(1+K_f)D_pM^{-1}(q)D_p^T > 0$ and hence is a P-matrix, the LCP (21) has a unique solution and one deduces that $\lambda_p > 0$ if and only if

$$\begin{aligned}
&\frac{\bar{M}_{p,p}(q)}{1+K_f}D_pM^{-1}(q)\big[U_{nc} - F(q,\dot{q}) - (1+K_f)D_p^T\,(\lambda_d)_p\big] < 0\\
&\Leftrightarrow (\lambda_d)_p > \frac{\bar{M}_{p,p}(q)}{1+K_f}D_pM^{-1}(q)\big[U_{nc} - F(q,\dot{q})\big]\\
&\Leftrightarrow (\lambda_d)_p = \beta + \frac{\bar{M}_{p,p}(q)}{1+K_f}D_pM^{-1}(q)\big[U_{nc} - F(q,\dot{q})\big] \qquad (22)
\end{aligned}$$

with $\beta \in \mathbb{R}^p$, $\beta > 0$. Since $U_{nc} - F(q,\dot{q}) = M(q)\ddot{q}_e - C(q,\dot{q})s - \gamma_1 s$, $(\ddot{q}_e)_p = 0$ and $s_p = 0$, (22) rewrites as (19) and the proof is finished. It is noteworthy that

$$\begin{aligned}
\lambda_p &= -\frac{\bar{M}_{p,p}(q)}{1+K_f}D_pM^{-1}(q)\big[U_{nc} - F(q,\dot{q}) - (1+K_f)D_p^T\,(\lambda_d)_p\big]\\
&= (\lambda_d)_p - \frac{\bar{M}_{p,p}(q)}{1+K_f}D_pM^{-1}(q)\big[U_{nc} - F(q,\dot{q})\big] = \beta
\end{aligned}$$

Remark 6 *The control law used in this paper with the design of λ_d described above leads to the following closed-loop dynamics on Ω_{2k+1}.*

$$\begin{cases}
M_{p,n-p}(q)\dot{s}_{n-p} + C_{p,n-p}(q,\dot{q})s_{n-p} = (1+K_f)(\lambda - \lambda_d)_p\\
M_{n-p,n-p}(q)\dot{s}_{n-p} + C_{n-p,n-p}(q,\dot{q})s_{n-p} + \gamma_1 s_{n-p} = 0\\
q_p = 0,\ \lambda_p = \beta
\end{cases}$$

It is noteworthy that the closed-loop dynamics is nonlinear and therefore, we do not use the feedback stabilization proposed in [15].

6 Strategy for take-off at the end of constraint phases Ω^J_{2k+1}

We have discussed in the previous sections the necessity of a trajectory with impacts in order to assure the robust stabilization on $\partial\Phi$ in finite time and, the design of the desired trajectory to stabilize the system on $\partial\Phi$. Now, we are interested in finding the conditions on the control signal U_c^J that assure the take-off at the end of constraint phases Ω^J_{2k+1}. As we have already seen before, the phase Ω^J_{2k+1} corresponds to the time interval $[t_f^k, t_d^k)$. The dynamics on $[t_f^k, t_d^k)$ is given by (18) and the system is permanently constrained, which implies $q_p(\cdot) = 0$ and $\dot{q}_p(\cdot) = 0$. Let us also consider that the first r constraints ($r < p$) have to be deactivated. Thus, the detachment takes place at t_d^k if $\ddot{q}_r(t_d^{k+}) > 0$ which requires $\lambda_r(t_d^{k-}) = 0$. The last $p - r$ constraints remain active which means $\lambda_{p-r}(t_d^{k-}) > 0$.

To simplify the notation we drop the time argument in many equations of this section. We decompose the LCP matrix (which is the Delassus' matrix multiplied by $1 + K_f$) as:

$$(1+K_f)D_pM^{-1}(q)D_p^T = \begin{pmatrix} A_1(q) & A_2(q)\\ A_2(q)^T & A_3(q)\end{pmatrix}$$

with $A_1 \in \mathbb{R}^{r\times r}$, $A_2 \in \mathbb{R}^{r\times(p-r)}$ and $A_3 \in \mathbb{R}^{(p-r)\times(p-r)}$

Proposition 3 *For the closed-loop system (18),(10),(12) the passage when the number of active constraints decreases from p to $r < p$, is possible if*

$$\begin{pmatrix} (\lambda_d)_r(t_d^k) \\ (\lambda_d)_{p-r}(t_d^k) \end{pmatrix} = \begin{pmatrix} \left(A_1 - A_2A_3^{-1}A_2^T\right)^{-1}\left(b_r - A_2A_3^{-1}b_{p-r}\right) - C_1 \\ C_2 + A_3^{-1}\left(b_{p-r} - A_2^T(\lambda_d)_r\right) \end{pmatrix} \tag{23}$$

where

$$b_p \triangleq b(q,\dot{q},U_{nc}) \triangleq D_pM^{-1}(q)[U_{nc} - F(q,\dot{q})] \geq 0$$

and $C_1 \in \mathbb{R}^r$, $C_2 \in \mathbb{R}^{p-r}$ such that $C_1 \geq 0$, $C_2 > 0$.

Proof: From (12) and (18) one gets

$$\ddot{q}_p(t) = b_p + (1+K_f)D_pM^{-1}(q)D_p^T(\lambda - \lambda_d)$$

Therefore the LCP (20) rewrites as:

$$0 \leq \begin{pmatrix} \lambda_r \\ \lambda_{p-r} \end{pmatrix} \perp \begin{pmatrix} b_r + A_1(\lambda-\lambda_d)_r + A_2(\lambda-\lambda_d)_{p-r} \\ b_{p-r} + A_2^T(\lambda-\lambda_d)_r + A_3(\lambda-\lambda_d)_{p-r} \end{pmatrix} \geq 0 \tag{24}$$

Under the conditions $\lambda_r = 0$ and $\lambda_{p-r} > 0$ one has

$$0 \leq \lambda_{p-r} \perp b_{p-r} - A_2^T(\lambda_d)_r + A_3(\lambda-\lambda_d)_{p-r} \geq 0$$

with the solution

$$\lambda_{p-r} = -A_3^{-1}\left(b_{p-r} - A_2^T(\lambda_d)_r - A_3(\lambda_d)_{p-r}\right) \tag{25}$$

Thus $\lambda_{p-r} > 0$ is equivalent to

$$(\lambda_d)_{p-r} > A_3^{-1}\left(b_{p-r} - A_2^T(\lambda_d)_r\right)$$

which leads to the second part of definition (23). Furthermore, replacing $(\lambda_d)_{p-r}$ in (25) we get $\lambda_{p-r} = C_2$ and $b_r + A_1(\lambda-\lambda_d)_r + A_2(\lambda-\lambda_d)_{p-r} \geq 0$ yields the first part of definition (23). To conclude, the solution of the LCP (24) is $\lambda_p = \begin{pmatrix} 0 \\ C_2 \end{pmatrix} \in \mathbb{R}^p$ and $(\lambda_d)_p$ is defined by (23).

Proposition 4 *The closed-loop system (18),(10),(12) is permanently constrained on $[t_f^k, t_d^k)$ and a smooth detachment is guaranteed on $[t_d^k, t_d^k + \epsilon)$ (ϵ is a small positive real number chosen by the designer) if*

(i) $(\lambda_d)_p(\cdot)$ *is defined on $[t_f^k, t_d^k)$ by (23) where C_1 is replaced by $C_1(t - t_d^k)$.*

(ii) On $[t_d^k, t_d^k + \epsilon)$

$$q_d^*(t) = q_d(t) = \begin{pmatrix} q_r^*(t) \\ q_{n-r}^{nc}(t) \end{pmatrix},$$

where $q_r^*(\cdot)$ is a twice differentiable function such that

$$\begin{array}{ll} q_r^*(t_d^k) = 0, & q_r^*(t_d^k+\epsilon) = q_r^{nc}(t_d^k+\epsilon), \\ \dot{q}_r^*(t_d^k) = 0, & \dot{q}_r^*(t_d^k+\epsilon) = \dot{q}_r^{nc}(t_d^k+\epsilon) \end{array} \tag{26}$$

and $\ddot{q}_r^*(t_d^{k+}) = a > \max\left(0,\ -A_1(q)(\lambda_d)_r(t_d^{k-})\right)$.

Proof: (i) The uniqueness of solution of the LCP (20) guarantees that (19) and (23) agree if $C_1 < 0$. In other words, replacing C_1 by $C_1(t - t_d^k)$ in (23) we assure a constrained motion on $[t_f^k, t_d^k)$ and the necessary conditions for detachment on $[t_d^k, t_d^k + \epsilon)$. (ii) Obviously (26) is imposed in order to assure the twice differentiability of the desired trajectory. Finally, straightforward computations show that

$$\sigma_{\ddot{q}_r(t_d^k)} = \ddot{q}_r^*(t_d^{k+}) + A_1(q)\,(\lambda_d)_r\,(t_d^{k-})$$

which means that the detachment is guaranteed and no other impacts occur when the desired acceleration satisfies $\ddot{q}_r^*(t_d^{k+}) > \max\left(0,\, -A_1(q)\,(\lambda_d)_r\,(t_d^{k-})\right)$.

7 Closed-loop stability analysis

In the case $\Phi = \mathbb{R}^n$, the function $V(t, s, \tilde{q})$ in (13) can be used in order to prove the closed-loop stability of the system (11), (12) (see for instance [6]). In the case studied here ($\Phi \subset \mathbb{R}^n$) the analysis becomes more complicated.

To simplify the notation $V(t, s(t), \tilde{q}(t))$ is denoted as $V(t)$. In order to introduce the main result of this paper we make the next assumption, which is verified in practice for dissipative systems.

Assumption 1 *The controller U_t in (12) assures that the sequence $\{t_\ell^k\}_{\ell \geq 0}$ of the impact times possesses a finite accumulation point t_∞^k i.e. $\lim_{\ell \to \infty} t_\ell^k = t_\infty^k < +\infty$, $\forall k$.*

It is worth to precise that during the stabilization on the intersection of p surfaces Σ_i we do not know which one and how many surfaces are stroked. However we assume that all the impacts are p_ϵ-impacts in the sense of Definition 3.

Lemma 1 *Consider the closed-loop system (10)-(12) with $(q_d^*)_p(\cdot)$ defined on the interval $[\tau_0^k, t_0^k]$ as in (14)-(16). Let us also suppose that condition* **b)** *of Proposition 1 is satisfied. The following inequalities hold:*

$$\begin{aligned} ||\tilde{q}(t_0^{k-})|| &\leq \sqrt{\frac{V(\tau_0^k)}{\gamma_1\gamma_2}},\; ||s(t_0^{k-})|| \leq \sqrt{\frac{2V(\tau_0^k)}{\lambda_{min}(M(q))}} \\ ||\dot{\tilde{q}}(t_0^{k-})|| &\leq \left(\sqrt{\frac{2}{\lambda_{min}(M(q))}} + \sqrt{\frac{\gamma_2}{\gamma_1}}\right) V^{1/2}(\tau_0^k) \end{aligned} \tag{27}$$

Furthermore, if $t_0^k \leq \tau_1^k$ one has

$$\begin{aligned} ||(q_d)_p(t_0^{k-})|| &\leq \epsilon + \sqrt{\frac{V(\tau_0^k)}{\gamma_1\gamma_2}} \\ ||(\dot{q}_d)_p(t_0^{k-})|| &\leq K + K' V^{1/6}(\tau_0^k) \end{aligned} \tag{28}$$

where ϵ is the real constant fixed in Definition 3 and $K,\ K' > 0$ are some constant real numbers that will be defined in the proof.

Proof: From (13) we can deduce on one hand that

$$V(t_0^{k-}) \geq \gamma_1\gamma_2 ||\tilde{q}(t_0^{k-})||^2$$

and on the other hand

$$V(t_0^{k-}) \geq \frac{1}{2} s(t_0^{k-})^T M(q(t_0^{k-})) s(t_0^{k-})$$

Since condition **b)** of Proposition 1 is satisfied one has $V(\tau_0^k) \geq V(t_0^{k-})$ and the first two inequalities in (27) become trivial. Let us recall that $s(t) = \dot{\tilde{q}}(t) + \gamma_2 \tilde{q}(t)$ which implies $||\dot{\tilde{q}}(t_0^{k-})|| \leq ||s(t_0^{k-})|| + \gamma_2 ||\tilde{q}(t_0^{k-})||$. Combining this with the first two inequalities in (27) we derive the third inequality in (27).
For the rest of the proof we assume that $t_0^k \leq \tau_1^k$. Therefore $(q_d)_p(t_0^{k-}) = (q_d^*)_p(t_0^k)$. It is clear that

$$||(q_d)_p(t_0^{k-})|| \leq ||\tilde{q}_p(t_0^{k-})|| + ||q_p(t_0^k)||$$

Taking into account that t_0^k is a p_ϵ-impact (which means $||q_p(t_0^k)|| \leq \epsilon$), the first inequality in (28) becomes obvious.
Let us denote $t'_k = \frac{t_0^k - \tau_0^k - \delta}{\tau_1^k - \tau_0^k - \delta} \in [0,1]$. We recall here that τ_0^k was chosen such that $||q_p^{nc}(\tau_0^k)|| \leq \psi$. From (14), (15) and the first inequality in (28), for $i = 1, \ldots, p$ one has

$$q_d^i(t_0^{k-}) = \left[(q^i)^{nc}(\tau_0^k) + \varphi V^{1/3}(\tau_0^k)\right] \left(2(t'_k)^3 - 3(t'_k)^2\right) + (q^i)^{nc}(\tau_0^k) \leq \epsilon + \sqrt{\frac{V(\tau_0^k)}{\gamma_1 \gamma_2}}$$

It follows that

$$3(t'_k)^2 - 2(t'_k)^3 \geq \frac{(q^i)^{nc}(\tau_0^k) - \epsilon - \sqrt{\frac{V(\tau_0^k)}{\gamma_1\gamma_2}}}{(q^i)^{nc}(\tau_0^k) + \varphi V^{1/3}(\tau_0^k)}$$

For $t > 0$ one has $2t - t^2 \geq 3t^2 - 2t^3$, therefore

$$2t'_k - (t'_k)^2 \geq \frac{(q^i)^{nc}(\tau_0^k) - \epsilon - \sqrt{\frac{V(\tau_0^k)}{\gamma_1\gamma_2}}}{(q^i)^{nc}(\tau_0^k) + \varphi V^{1/3}(\tau_0^k)}$$

which means that

$$(1 - t'_k)^2 \leq \frac{\sqrt{\frac{V(\tau_0^k)}{\gamma_1\gamma_2}} + \varphi V^{1/3}(\tau_0^k) + \epsilon}{(q^i)^{nc}(\tau_0^k) + \varphi V^{1/3}(\tau_0^k)}$$

Straightforward computations lead to

$$|\dot{q}_d^i(t_0^{k-})| = \frac{6((q^i)^{nc}(\tau_0^k) + \varphi V^{1/3}(\tau_0^k))}{\tau_1^k - \tau_0^k - \delta} \left(t'_k - (t'_k)^2\right)$$

Since $t'_k - (t'_k)^2 \leq 1 - t'_k$ and $(q^i)^{nc}(\tau_0^k) \leq \psi$, one arrives at (see Appendix 10.1 for details)

$$|\dot{q}_d^i(t_0^{k-})| \leq \frac{6\sqrt{\psi\epsilon}}{\tau_1^k - \tau_0^k - \delta} + \frac{6\sqrt{\left(\frac{1}{\sqrt{\gamma_1\gamma_2}} + \varphi\right)(\varphi + \psi) + \epsilon\varphi}}{\tau_1^k - \tau_0^k - \delta} V^{1/6}(\tau_0^k) \qquad (29)$$

Therefore, the second inequality in (28) holds with

$$K = \frac{6\sqrt{p\psi\epsilon}}{\tau_1^k - \tau_0^k - \delta}, \quad K' = \frac{6\sqrt{p}}{\tau_1^k - \tau_0^k - \delta} \sqrt{\left(\frac{1}{\sqrt{\gamma_1\gamma_2}} + \varphi\right)(\varphi + \psi) + \epsilon\varphi}$$

We now state the main result of this paper.

Theorem 1 *Let Assumption 1 hold, $e \in [0,1)$ and $(q_d^*)_p$ defined as in (14)-(16). The closed-loop system (10)-(12) initialized on Ω_0 such that $V(\tau_0^0) \leq 1$, satisfies the requirements of Proposition 1 and is therefore practically weakly stable with the closed-loop state $x(\cdot) = [s(\cdot), \tilde{q}(\cdot)]$ and $R = \sqrt{e^{-\gamma(t_f^k - t_\infty^k)}(1 + K_1 + K_2 + \xi)/\rho}$ where $\rho = \min\{\lambda_{min}(M(q))/2; \gamma_1\gamma_2\}$.*

Proof: First we observe that conditions **a)** and **d)** of Proposition 1 hold when the hypothesis of the Theorem are verified. Thus in order to prove Theorem 1 it is sufficient to verify the conditions **b)**, **c)** and **e)** of Proposition 1. It is noteworthy that during the transition phases $I_k^{J_k}$ some p_ϵ–impact occurs (according to (8) we have $J_k' = \{1, \ldots, p\}$). This means that we do not know which and how many of them are the constraints touched at each contact. However, in the neighborhood of the desired stabilization point situated on a surface of codimension p, only the corresponding p constraints enter the dynamics. In the sequel we shall also use the function $V_1(t,s) = \frac{1}{2}s(t)^T M(q)s(t)$.
b) Using that $\dot{M}(q) - 2C(q,\dot{q}))$ is a skew-symmetric matrix, straightforward computations show that on $\mathbb{R}_+ \setminus \bigcup_{k\geq 0}[t_0^k, t_f^k]$ the time derivative of the Lyapunov function is given by

$$\dot{V}(t) = -\gamma_1 s^T s + 2\gamma_1\gamma_2 \tilde{q}^T \dot{\tilde{q}} = -\gamma_1 ||\dot{\tilde{q}}||^2 - \gamma_1\gamma_2^2 ||\tilde{q}||^2$$

On the other hand

$$V(t) \leq \frac{\lambda_{max}(M(q))}{2}||s||^2 + \gamma_1\gamma_2||\tilde{q}||^2 \leq \gamma^{-1}[\gamma_1||\dot{\tilde{q}}||^2 + \gamma_1\gamma_2^2||\tilde{q}||^2]$$

where

$$\gamma^{-1} = \max\left\{\lambda_{max}(M(q))\frac{1+2\gamma_2}{2\gamma_1}; \frac{\lambda_{max}(M(q))(\gamma_2+2)+2\gamma_1}{2\gamma_1\gamma_2}\right\} > 0$$

Therefore $\dot{V}(t) \leq -\gamma^{-1}V(t)$ on $\mathbb{R}_+ \setminus \bigcup_{k\geq 0}[t_0^k, t_f^k]$.
c) By definition

$$V(t_{\ell+1}^{k-}) - V(t_\ell^{k+}) = V_1(t_{\ell+1}^{k-}) - V_1(t_\ell^{k+}) + \gamma_1\gamma_2[(\tilde{q}^T(t_{\ell+1}^{k-}))\tilde{q}(t_{\ell+1}^{k-}) - (\tilde{q}^T(t_\ell^{k+}))\tilde{q}(t_\ell^{k+})] \tag{30}$$

On the other hand, straightforward computations show that

$$\begin{aligned} V_1(t_{\ell+1}^{k-}) - V_1(t_\ell^{k+}) = \int_{(t_\ell^k, t_{\ell+1}^k)} \dot{V}_1(t)\mathrm{d}t &= \gamma_1\gamma_2 \int_{(t_\ell^k, t_{\ell+1}^k)} s_p^T(t)(q_d^*)_p(t)\mathrm{d}t \\ &\quad - \gamma_1 \int_{(t_\ell^k, t_{\ell+1}^k)} s(t)^T s(t)\mathrm{d}t \end{aligned} \tag{31}$$

Furthermore,

$$\begin{aligned} \int_{(t_\ell^k, t_{\ell+1}^k)} s(t)^T s(t)\mathrm{d}t = \int_{(t_\ell^k, t_{\ell+1}^k)} &||\dot{\tilde{q}}(t)||^2 + \gamma_2^2||\tilde{q}(t)||^2\mathrm{d}t + \gamma_2[(\tilde{q}^T(t_{\ell+1}^{k-}))\tilde{q}(t_{\ell+1}^{k-}) \\ &- (\tilde{q}^T(t_\ell^{k+}))\tilde{q}(t_\ell^{k+})] \end{aligned} \tag{32}$$

Therefore, inserting successively (32) in (31) and (31) in (30) one arrives at

$$V(t_{\ell+1}^{k-}) - V(t_\ell^{k+}) \leq \gamma_1\gamma_2 \int_{(t_\ell^k, t_{\ell+1}^k)} s_p^T(t)(q_d^*)_p(t)\mathrm{d}t \tag{33}$$

In the sequel let us denote by $S(q)$ the sum of all the components of the vector q. Taking into account the definition (14) and the fact that $(q_d)_p$ and $(\dot{q}_d)_p$ are set to zero at t_0^{k+} one obtains

$$\int_{(t_\ell^k, t_{\ell+1}^k)} s_p^T(t)(q_d^*)_p(t)\mathrm{d}t = -\varphi V^{1/3}(\tau_0^k) \cdot \left(\int_{(t_\ell^k, t_{\ell+1}^k)} S(\dot{q}_p(t))\mathrm{d}t + \gamma_2 \int_{(t_\ell^k, t_{\ell+1}^k)} S(q_p(t))\mathrm{d}t \right)$$

Since $\varphi\gamma_2 V^{1/3}(\tau_0^k) \geq 0$ and $S(q_p(t)) \geq 0$ it follows that

$$\int_{t_\ell^k}^{t_{\ell+1}^k} s_p^T(t)(q_d^*)_p(t)\mathrm{d}t \leq \varphi V^{1/3}(\tau_0^k)[S(q_p(t_\ell^k)) - S(q_p(t_{\ell+1}^k))]$$

Thus

$$\sum_{\ell \geq 0} \left[V(t_{\ell+1}^{k-}) - V(t_\ell^{k+}) \right] \leq \gamma_1\gamma_2\varphi V^{1/3}(\tau_0^k) S(q_p(t_0^k)) \leq \gamma_1\gamma_2\varphi V^{1/3}(\tau_0^k)\sqrt{3}||q_p(t_0^k)||$$

Recalling that t_0^k is an p_ϵ-impact which means that $||q_p(t_0^k)|| \leq \epsilon$ one obtains

$$\sum_{\ell \geq 0} \left[V(t_{\ell+1}^{k-}) - V(t_\ell^{k+}) \right] \leq K_1 V^{p_1}(\tau_0^k)$$

where $K_1 = \sqrt{3}\gamma_1\gamma_2\varphi\epsilon > 0$ and $p_1 = \frac{2}{3}$.

e) First, let us compute the Lyapunov function's jumps at the instants t_ℓ^k, $\ell \geq 1$. Using the continuity of the real trajectory $q(\cdot)$ and the definition of the desired trajectory $q_d(\cdot)$ on the I_k phases (i.e. $q_d(t_\ell^{k+}) = q_d(t_\ell^{k-})$, $\dot{q}_d(t_\ell^{k+}) = 0 = \dot{q}_d(t_\ell^{k-})$) one gets

$$\begin{aligned} \sigma_V(t_\ell^k) &= V(t_\ell^{k+}) - V(t_\ell^{k-}) \\ &= \gamma_1\gamma_2\sigma_{||\tilde{q}||^2}(t_\ell^k) + \frac{s^T(t_\ell^{k+})M_\ell s(t_\ell^{k+}) - s^T(t_\ell^{k-})M_\ell s(t_\ell^{k-})}{2} \\ &= T_L(t_\ell^k) + \gamma_2\tilde{q}(t_\ell^k)^T M_\ell \sigma_{\dot{q}}(t_\ell^k) \end{aligned} \tag{34}$$

where M_ℓ^k denotes the inertia matrix $M(q(t_\ell^k))$ and T_L is the kinetic energy loss at the impact time t_ℓ^k. From equation (5) one has $T_L(t_\ell^k) \leq 0$ and equation (34) becomes $\sigma_V(t_\ell^k) \leq \gamma_2\tilde{q}(t_\ell^k)^T M_\ell \sigma_{\dot{q}}(t_\ell^k)$. Let us recall that $M_\ell\sigma_{\dot{q}}(t_\ell^k)$ is the percussion vector (see [5]). On the other hand in the X coordinates the percussion vector can be expressed as $\nabla F(X)\lambda$. Writing the latter in the generalized coordinates introduced in Section 3 one obtains $M_\ell\sigma_{\dot{q}}(t_\ell^k) = D^T\lambda$. In other words the generalized coordinates introduced in Section 3 coincide with the so called quasi-coordinates and the vector $\dot{q}_{tang}$ is in fact $\dot{q}_{n-m}$ (i.e. $\sigma_{\dot{q}}(t_\ell^k) = \begin{pmatrix} \sigma_{\dot{q}_m}(t_\ell^k) \\ \mathbf{0}_{n-m} \end{pmatrix}$ where $\mathbf{0}_{n-m}$ denotes the $n-m$ vector with all its components equal zero). Therefore

$$\sigma_V(t_\ell^k) \leq \gamma_2\tilde{q}(t_\ell^k)^T M_\ell \sigma_{\dot{q}}(t_\ell^k) = \gamma_2 q_p(t_\ell^k)^T \lambda_p = 0 \tag{35}$$

where we have used $(q_d)_p(t_\ell^{k+}) = 0 = (q_d)_p(t_\ell^{k-})$ and the last equality is stated using the complementarity relation entering the dynamics.

The Lyapunov function's jump corresponding to the first impact of each cycle can be computed as:

$$\begin{aligned}\sigma_V(t_0^k) &= V(t_0^{k+}) - V(t_0^{k-}) \\ &= \gamma_1\gamma_2\sigma_{||\tilde{q}||^2}(t_0^k) + \frac{s^T(t_0^{k+})M_0 s(t_0^{k+}) - s^T(t_0^{k-})M_0 s(t_0^{k-})}{2}\end{aligned} \tag{36}$$

- It is clear that $t_0^k > \tau_1^k$ implies $q_d(t_0^{k+}) = q_d(t_0^{k-})$ and $\dot{q}_d(t_0^{k+}) = 0 = \dot{q}_d(t_0^{k-})$. Thus, the computations for $t_\ell^k,\ \ell \geq 1$ hold also for t_0^k.
- If $t_0^k \leq \tau_1^k$ one has $(q_d)_p(t_0^{k-}) \neq (q_d)_p(t_0^{k+}) = 0$ and $(\dot{q}_d)_p(t_0^{k-}) \neq (\dot{q}_d)_p(t_0^{k+}) = 0$. Then the initial jump of each cycle is given by:

$$\begin{aligned}\sigma_V(t_0^k) &= \dot{q}_d(t_0^{k-})^T M_0 \dot{q}(t_0^{k-}) + \frac{\gamma_2^2}{2}\left(\tilde{q}(t_0^{k+})^T M_0 \tilde{q}(t_0^{k+}) - \tilde{q}(t_0^{k-})^T M_0 \tilde{q}(t_0^{k-})\right) \\ &+ \gamma_2\left(\dot{q}(t_0^{k+})^T M_0 \tilde{q}(t_0^{k+}) - \dot{\tilde{q}}(t_0^{k-})^T M_0 \tilde{q}(t_0^{k-})\right) - \frac{1}{2}\dot{q}_d(t_0^{k-})^T M_0 \dot{q}_d(t_0^{k-}) + T_L(t_0^k)\end{aligned} \tag{37}$$

Since $T_L(t_0^k) \leq 0$ the equation (37) rewrites as:

$$\begin{aligned}\sigma_V(t_0^k) &\leq \lambda_{max}(M(q))\Big[\gamma_2\left(||(\dot{q}_d)_p(t_0^{k-})|| \cdot ||\tilde{q}(t_0^{k-})|| + ||\dot{q}(t_0^{k-})|| \cdot ||(q_d)_p(t_0^{k-})||\right) \\ &+ \frac{\gamma_2^2}{2}\left(||q_p(t_0^k)||^2 + ||\tilde{q}_p(t_0^{k-})||^2 + 2||(q_d)_p(t_0^{k-})|| \cdot ||\tilde{q}_{n-p}(t_0^{k-})||\right) \\ &+ \frac{1}{2}||(\dot{q}_d)_p(t_0^{k-})||^2 + ||(\dot{q}_d)_p(t_0^{k-})|| \cdot ||\dot{q}(t_0^{k-})||\Big]\end{aligned} \tag{38}$$

Obviously $||\dot{q}(t_0^{k-})|| = ||\dot{\tilde{q}}(t_0^{k-}) + (\dot{q}_d)_p(t_0^{k-})||$ and Lemma 1 combined with $V(\tau_0^k) < 1$ yields

$$||\dot{q}(t_0^{k-})|| \leq K + \left(\sqrt{\frac{2}{\lambda_{min}(M)}} + \sqrt{\frac{\gamma_2}{\gamma_1}} + K'\right) V^{1/6}(\tau_0^k)$$

Therefore

$$\sigma_V(t_0^k) \leq K_2 V^{p_2}(\tau_0^k) + \xi$$

where $p_2 = \frac{1}{6}$, $\xi = \frac{3}{2}K^2 + \gamma_2\epsilon K + \frac{\gamma_2^2\epsilon^2}{2}$ and

$$\begin{aligned}K_2 = \lambda_{max}(M(q))\Bigg[&3KK' + \frac{3}{2}(K')^2 + \frac{\gamma_2}{2}\sqrt{\frac{\gamma_2}{\gamma_1}} + \sqrt{\frac{2\gamma_2}{\lambda_{min}(M(q))\gamma_1}} + \frac{2\gamma_2}{\gamma_1} \\ &+ (K' + K)\left(3\sqrt{\frac{\gamma_2}{\gamma_1}} + \sqrt{\frac{2}{\lambda_{min}(M(q))}}\right) + \epsilon\gamma_2\left(2\sqrt{\frac{\gamma_2}{\gamma_1}} + \sqrt{\frac{2}{\lambda_{min}(M(q))}} + K'\right)\Bigg]\end{aligned}$$

Defining $\alpha : \mathbb{R}_+ \mapsto \mathbb{R}_+$, $\alpha(\omega) = \rho\omega^2$ we get $\alpha(0) = 0$ and $\alpha(|||[s(t), \tilde{q}(t)]|||) \leq V(t, s, \tilde{q})$. Thus, Proposition 1 also yields

$$R = \alpha^{-1}(e^{-\gamma(t_f^k - t_\infty^k)}(1 + K_1 + K_2 + \xi)) = \sqrt{e^{-\gamma(t_f^k - t_\infty^k)}(1 + K_1 + K_2 + \xi)/\rho}$$

which ends the proof.

8 Illustrative example

The main issues of the control scheme proposed in this paper are emphasized simulating the behavior of a planar two-link rigid-joint manipulator in presence of one unilateral constraint.

8.1 Dynamics Equation based on Lagrangian formulation

First, we will derive the dynamics of a two-link manipulator moving in the XOY plane. In order to accomplish our goal let us introduce the following notations (see Figure 5):

- θ_i - the joint angle of the joint i,
- m_i - the mass of link i,
- I_i - the moment of inertia of link i about the axis that passes through the center of mass and is parallel to the Z axis,
- l_i - the length of link i,
- g - the gravitational acceleration.

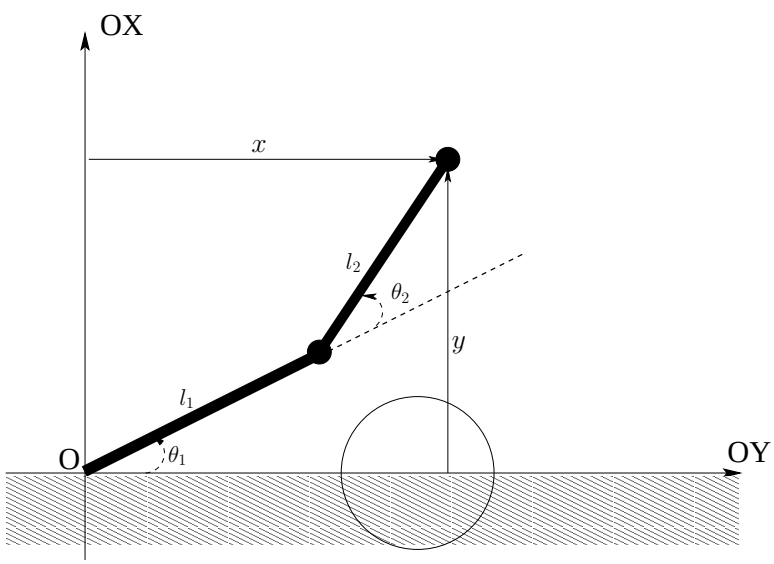

Figure 5: Two-link planar manipulator

For the sake of simplicity we assume that the center of mass of each link is right at the middle of the link. We will also assume that the gravitational force acts in the negative direction of the Y axis.

First, let us choose $\theta = (\theta_1, \theta_2)^T$ as the generalized coordinates and denote T the kinetic energy, P the potential energy and $L = T - P$ the Lagrangian function. Using the above notations, the potential and the kinetic energies of the system can be

expressed as follows:

$$\begin{aligned} P &= \frac{1}{2}m_1 g l_1 \sin\theta_1 + m_2 g\left(l_1\sin\theta_1 + \frac{l_2}{2}\sin(\theta_1+\theta_2)\right), \\ T &= \frac{m_1 l_1^2 \dot{\theta_1}^2}{8} + \frac{m_2}{2}\left(l_1^2\dot{\theta}_1^2 + \frac{l_2^2}{4}(\dot{\theta}_1+\dot{\theta}_2)^2 + l_1 l_2(\dot{\theta}_1^2+\dot{\theta}_1\dot{\theta}_2)\cos\theta_2\right) \\ &+ \frac{I_1\dot{\theta_1}^2 + I_2(\dot{\theta_1} + \ dot\theta_2)^2}{2}. \end{aligned}$$

Substituting P and T in the formula of L the dynamical equation of the two-links manipulator:

$$\frac{\mathrm{d}}{\mathrm{d}t}\left(\frac{\partial L}{\partial\dot{\theta}}\right) - \frac{\partial L}{\partial\theta} = 0$$

can be rewritten as

$$M(\theta)\ddot{\theta} + C(\theta,\dot{\theta})\dot{\theta} + G(\theta) = 0 \tag{39}$$

where $M, C \in \mathbb{R}^{2\times 2}, G \in \mathbb{R}^2$ have the same meaning as in (1) and they are explicitly given by:

$$M = \begin{bmatrix} M_{11} & M_{12} \\ M_{21} & M_{22} \end{bmatrix}, \qquad \begin{cases} M_{11} &= \frac{m_1 l_1^2}{4} + m_2\left(l_1^2 + \frac{l_2^2}{4}l_1 l_2\cos\theta_2\right) + I_1 + I_2 \\ M_{12} &= M_{21} = \frac{m_2 l_2^2}{4} + \frac{m_2 l_1 l_2}{2}\cos\theta_2 + I_2 \\ M_{22} &= \frac{m_2 l_2^2}{4} + I_2 \end{cases}$$

$$C = \begin{bmatrix} C_{11} & C_{12} \\ C_{21} & C_{22} \end{bmatrix}, \qquad \begin{cases} C_{11} &= -m_2 l_1 l_2 \dot{\theta}_2 \sin\theta_2 \\ C_{12} &= -\frac{m_2 l_1 l_2}{2}\dot{\theta}_2\sin\theta_2 \\ C_{21} &= \frac{m_2 l_1 l_2}{2}\dot{\theta}_1\sin\theta_2 \\ C_{22} &= 0 \end{cases}$$

$$G = \begin{bmatrix} G_1 \\ G_1 \end{bmatrix}, \qquad \begin{cases} G_1 &= \frac{g}{2}[l_1(2m_1+m_2)\cos\theta_1 + m_2 l_2\cos(\theta_1+\theta_2)] \\ G_2 &= \frac{m_2 g l_2}{2}\cos(\theta_1+\theta_2) \end{cases}$$

The admissible domain is the upper half plane $y \geq 0$ and the unconstrained desired trajectory $q^{nc}(\cdot)$ is given by a circle that violates the constraint. Precisely, the end effector must follow a half-circle, stabilize on the constraint ($y = 0$) and move on the constraint until the point where the circle $q^{nc}(\cdot)$ re-enters the admissible domain. The lengths l_1, l_2 of the manipulator's links are set to $0.5m$, and their masses m_1, m_2 are set to $1kg$. The impacts are imposed using the parameter $\varphi = 100$ in (14)-(15).

8.2 Some remarks concerning the simulation scheme

The numerical simulations are done with the Moreau's time-stepping algorithm of the SICONOS software platform [2]. The choice of a time-stepping algorithm was mainly dictated by the presence of accumulations of impacts which render the use of event-driven methods difficult [1].

Let us set $e = 0.7$, $\gamma_1 = 8$, $\gamma_2 = 7$, 10 seconds the period of each cycle and 30 seconds the final simulation time. First, let us point out (Figure 6 (left)) the influence of ψ (i.e.

the choice of τ_0^k) on the degree of deformation of the real trajectory w.r.t. the desired unconstrained one. As we have pointed out in Section 4 the deformation gets smaller when $\psi > 0$ decreases. It is noteworthy that the tangential approach corresponding to $\psi = 0$ lacks of robustness and is unreliable due to the nonzero initial tracking errors.

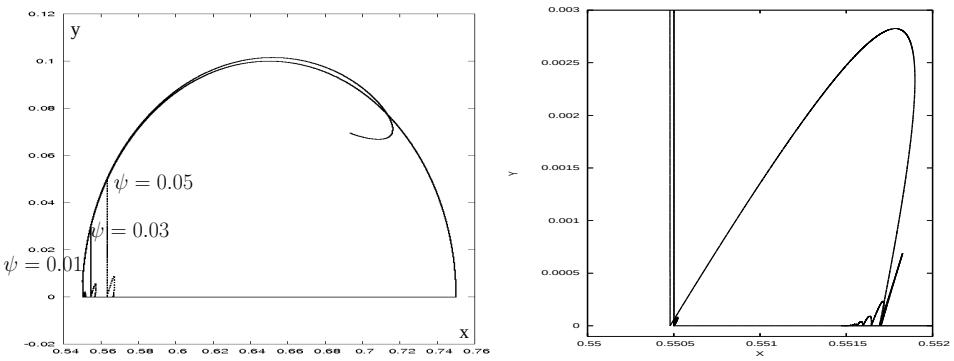

Figure 6: Left: The influence of ψ on the real trajectory's deformation for controller's gains set to $\gamma_1 = 8$, $\gamma_2 = 7$. Right: The trajectory of the end-effector on the transition phases when $\psi = 0.1$.

For $\psi = 0.01$ in Figure 6 (right) we illustrate the trajectory of the system during the stabilization on $\partial\Phi = \{(x, y) \mid y = 0\}$. The switches of the controller during the first cycle are depicted in Figure 7 (left). Clearly since the velocity jumps, the controller jumps as well.

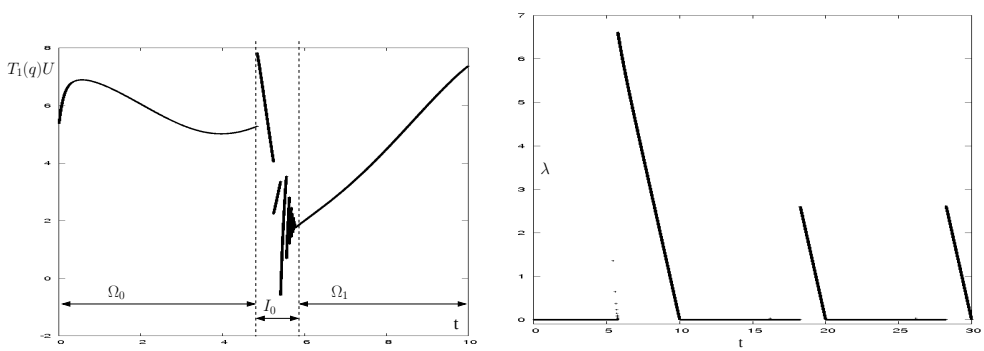

Figure 7: Left: The switching controller on the first cycle; Right: Variation of the contact force λ

The Figure 7 (right) presents the variation of the contact force λ. Precisely, one sees that λ remains 0 during the free motion phases and it points out each impact during transients (better seen on I_0 since the impacts are more violent). The contact force λ is designed as a decreasing linear function during constrained motion phases Ω_{2k+1} in order to allow a smooth detachment at the end of these phases. It is worth to mention that the magnitude of λ depends indirectly on $V(\tau_0^k)$. Precisely, when $V(\tau_0^k)$ approaches zero the system tends to a tangential stabilization on $\partial\Phi$ which implies larger values of t_0^k and consequently smaller length of $[t_f^k, t_d^k]$ and smaller magnitude of the contact force measured by λ (see Proposition 4).

Figure 8 shows that the tracking error described by the Lyapunov function rapidly decreases and remains close to 0. In other words the practical weak stability is guaranteed. On the zoom made in Figure 8 one can also observe the behavior of $V(\cdot)$ during the stabilization on $\partial\Phi$, that is an almost decreasing function.

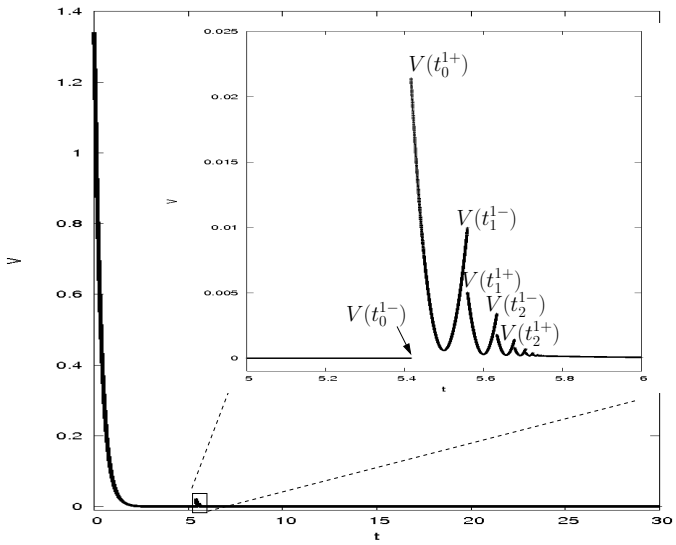

Figure 8: Variation of the Lyapunov function for $\gamma_1 = 8, \gamma_2 = 7$; Zoom: Variation of the Lyapunov function during the phase I_0

8.3 The influence of the time-step on the closed-loop dynamics

It is noteworthy that the simulation results do not depend essentially on the time-step chosen for the scheme (since the Moreau's time-stepping algorithm converges [8]) but, a smaller time-step allows to capture more precisely the behavior of the system. On the other hand, as can be seen in figure 9 the real trajectory and the lengths of each transition phase are almost unchanged starting with a sufficiently small time-step ($h = 10^{-3}$).

We do not insist too much on the simulation results during free-motion phases since the smoothness of the system is guaranteed on these phases and the behavior of the system is clear. The most interesting phases from the numerical point of view are the transition (accumulation of impacts) phases. It is worth to clarify that the number of impacts during the transition phases is not so important and the major issue is the finiteness of these phases. To be more clear, in the next tables we summarize some numerical results when $\psi = 0.01$, $e = 0.7$, $\gamma_1 = 35$, $\gamma_2 = 20$. The period of each cycle is set to 5 seconds and the final simulation time rest 30 seconds. First, one can see that the length of the transition phase I_0 with respect to the time-step h does not vary significantly when the time-step decreases. Let us also denote by CPU the computing time necessary for the simulation (using an Intel(R) Core(TM)2 CPU 6300 1.86GHz) of one cycle.

h	$10^{-3}s$	$10^{-4}s$	$10^{-5}s$	$10^{-6}s$
$\lambda[I_0]$	0.945	0.9536	0.9525	0.9523
CPU	$1.5s$	$11.2s$	$111.3s$	$1072.2s$

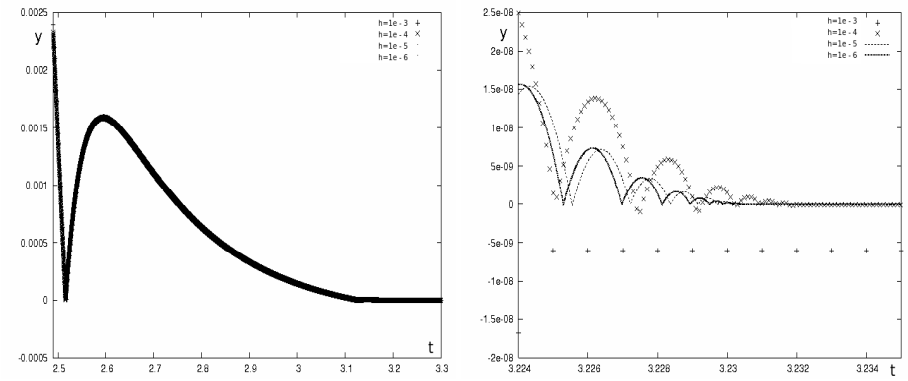

Figure 9: Left: The variation of q_1 during transition phase for $h \in \{10^{-3},\ 10^{-4},\ 10^{-5},\ 10^{-6}\}$; Right: Zoom at the end of transition phase.

The evolutions of the number of impacts n_i w.r.t. the restitution coefficient e and the time-step h are quite different. As expected, n_i becomes larger when the restitution coefficient increases. Also, one can see that the accumulation of impacts can be captured with a higher precision when the time-step becomes smaller.

$e \setminus h$	$10^{-3}s$	$10^{-4}s$	$10^{-5}s$	$10^{-6}s$
0.2	$n_i = 3$	$n_i = 5$	$n_i = 6$	$n_i = 8$
0.5	$n_i = 6$	$n_i = 9$	$n_i = 12$	$n_i = 16$
0.7	$n_i = 9$	$n_i = 16$	$n_i = 23$	$n_i = 29$
0.9	$n_i = 23$	$n_i = 40$	$n_i = 64$	$n_i = 81$
0.95	$n_i = 32$	$n_i = 67$	$n_i = 108$	$n_i = 161$

However, a larger number of captured impacts does not change the global behavior of the simulated system and the transition phase ends almost in the same moment when h varies, see $\lambda[I_0]$ in the first table.

In conclusion, reliable simulations with a reasonable CPU time can be performed with the Moreau's time-stepping scheme of the SICONOS *platform, with a time-step $h = 10^{-4}s$.*

8.4 The influence of controller parameters on the closed-loop dynamics

In this paragraph we present several simulations with different values of the controller parameters in order to see their influence on the closed-loop dynamics. Some intuitive explanation will join the numerical results presented in the following. It is worth to precise that we keep for the next simulations a period of 5 seconds for each cycle and we fix the time-step at the value of 10^{-4} seconds.

In order to explain more easily the results of this section we point out from the beginning that γ_1 is the coefficient of the velocity error and $\gamma_1\gamma_2$ is the coefficient of the position error entering both in the controller and the Lyapunov function.

First one considers a fixed value of $\gamma_1 = 25$ and one studies the behavior of the closed-loop dynamics w.r.t. γ_2 variation. The main influence in this case can be seen during the transition phases I_k. More precisely, the Figure 10 shows that diminishing the value of γ_2 the transition phases get larger. From a mechanical point of view

decreasing γ_2 one decreases the stiffness of the spring entering the controller and therefore we get more jumps, higher first jump (see Figure 10 (right)) and longer transition phases. Obviously, this may lead to the system's instability (as can be seen in Figure 10 (left) for $\gamma_2 = 2$).

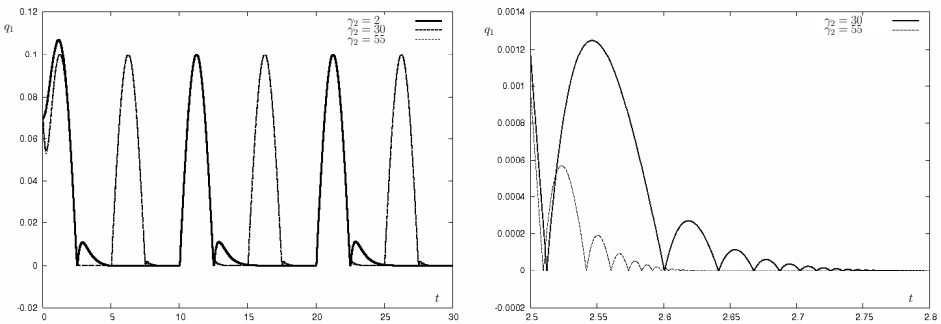

Figure 10: Left: The variation of $q_1(t)$ during 6 cycles for $\gamma_2 \in \{2,\ 30,\ 55\}$; Right: The variation of $q_1(t)$ during I_0 for $\gamma_2 \in \{30,\ 55\}$.

The above discussion is also illustrated in the next table where we denote by H the height of the first jump.

γ_2	2	30	55
n_i	101	65	58
H	0.01091	0.00124	0.00056
$\lambda[I_0]$	4.088	0.313	0.148

Next one considers a fixed value of $\gamma_1\gamma_2 = 800$ and we repeat the simulation for different value of γ_1. From mechanical point of view, this means that we fix the spring stiffness entering the controller and we point out the effect of the damper gain on the system dynamics. Precisely, decreasing the value of γ_1 we detect an increasing tracking error, see figure 11. In other words, the real trajectory approaches slower the desired trajectory.

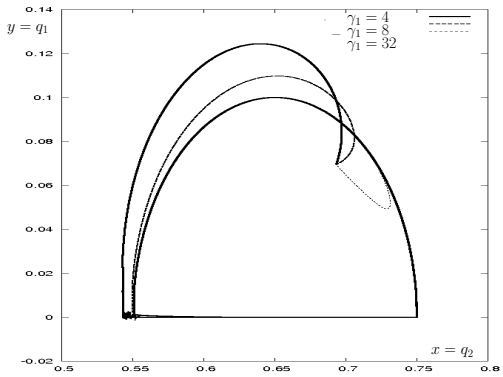

Figure 11: Smaller values of γ_1 lead to larger tracking errors.

In the sequel we want to emphasize the behavior of the system during each phase of the motion. Let us consider the spring stiffness $\gamma_1\gamma_2 = 5$ and the damper gain $\gamma_1 = 10$.

Taking into account the response of the system to the variation of the spring stiffness and damper gain entering the controller this choice leads to one of the worst possible situation (small convergence speed, high jumps and long transients). In order to compensate the bad choice of controller gains we consider a low value of the restitution coefficient $e = 0.3$ and, since the initial tracking errors are relatively big, the impacts are imposed using a smaller parameter $\varphi = 10$ in (14)-(15). However, the high jumps and the small convergence speed allows to better identify each particular phase of the motion (see Figure 12 (left)). On the other hand, as depicted in Figure 12 (right), the accumulation of impacts phases are too long and the end-effector cannot accomplish its task in the fixed period set to 5 seconds. It is noteworthy that large values of spring stiffness and dumper gain improve the tracking control leading to an "almost tangential" contact. Nevertheless, as pointed out before, a tangential contact is not desired due to its unreliability.

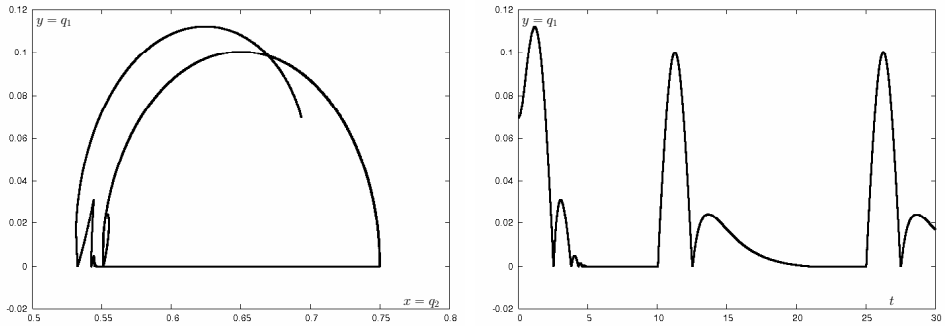

Figure 12: Left: The system trajectory in the xOy-plane for $\gamma_1 = 10$ and $\gamma_2 = 0.5$; Right: The variation of $q_1(t)$ for $\gamma_1 = 10$ and $\gamma_2 = 0.5$.

9 Conclusions

In this paper we have proposed a methodology to study the tracking control of fully actuated Lagrangian systems subject to multiple frictionless unilateral constraints. The main contribution of the work is twofold: first, it formulates a general framework and second, it provides a complete stability analysis for the class of systems under consideration. It is noteworthy that even in the case of only one frictionless unilateral constraint the paper presents some improvements with respect to the existing works in the literature. Precisely, the stability analysis result is significantly more general than those presented in [4] and [7] and, each element entering the dynamics (desired trajectory, contact force) is explicitly defined. Numerical simulations are done with the SICONOS software platform [1, 2] in order to illustrate the results.

10 Appendix

10.1 Computation details for inequality (29)

In order to prove inequality (29) we recall that

$$1 - t'_k \leq \sqrt{\frac{\sqrt{\frac{V(\tau_0^k)}{\gamma_1\gamma_2}} + \varphi V^{1/3}(\tau_0^k) + \epsilon}{(q^i)^{nc}(\tau_0^k) + \varphi V^{1/3}(\tau_0^k)}}$$

and

$$|\dot{q}_d^i(t_0^{k-})| = \frac{6((q^i)^{nc}(\tau_0^k) + \varphi V^{1/3}(\tau_0^k))}{\tau_1^k - \tau_0^k - \delta}\left(t'_k - (t'_k)^2\right)$$

Since $t'_k - (t'_k)^2 \leq 1 - t'_k$ and $(q^i)^{nc}(\tau_0^k) \leq \psi$ one has

$$\begin{aligned}
|\dot{q}_d^i(t_0^{k-})| &\leq \frac{6((q^i)^{nc}(\tau_0^k) + \varphi V^{1/3}(\tau_0^k))}{\tau_1^k - \tau_0^k - \delta}(1 - t'_k) \\
&\leq \frac{6}{\tau_1^k - \tau_0^k - \delta}\sqrt{(\psi + \varphi V^{1/3}(\tau_0^k))\left(\sqrt{\frac{V(\tau_0^k)}{\gamma_1\gamma_2}} + \varphi V^{1/3}(\tau_0^k) + \epsilon\right)} \\
&= \frac{6\sqrt{\psi\epsilon + (\psi\varphi + \epsilon\varphi)V^{1/3}(\tau_0^k) + \varphi^2 V^{2/3}(\tau_0^k) + \frac{\varphi V^{5/6}(\tau_0^k) + \psi V^{1/2}(\tau_0^k)}{\sqrt{\gamma_1\gamma_2}}}}{\tau_1^k - \tau_0^k - \delta}
\end{aligned}$$

Since $V(\tau_0^k) < 1$ (thus $V^{p_1}(\tau_0^k) > V^{p_2}(\tau_0^k)$ for $p_1 < p_2$) one obtains

$$|\dot{q}_d^i(t_0^{k-})| \leq \frac{6}{\tau_1^k - \tau_0^k - \delta} \times \sqrt{\psi\epsilon + \left[\left(\frac{1}{\sqrt{\gamma_1\gamma_2}} + \varphi\right)(\varphi + \psi) + \epsilon\varphi\right] V^{1/3}(\tau_0^k)}$$

which leads to (29).

References

[1] Acary, V. and Brogliato, B.: *Numerical Methods for Nonsmooth Dynamical Systems*, Lecture Notes in Applied and Computational Mechanics, vol **35**, Springer-Verlag, Berlin Heidelberg, (2008).

[2] Acary, V. and Pérignon, F.: *An introduction to* SICONOS, INRIA Technical report RT 340, (2007) SICONOS open-source software available at: http://siconos.gforge.inria.fr/.

[3] Ballard, P.: *Formulation and well-posedness of the dynamics of rigid body systems with perfect unilateral constraints*, Phil. Trans. R. Soc. Lond. **A359**, 2327-2346, (2001).

[4] Bourgeot, J.-M. and Brogliato, B.:*Tracking control of complementarity lagrangian systems*, International Journal of Bifurcation and Chaos, **15**(6), 1839-1866, (2005).

[5] Brogliato, B.: *Nonsmooth Mechanics*, Springer CCES, London, (1999), 2nd Ed.

[6] Brogliato, B., Lozano, R., Maschke, B. and Egeland, O.: *Dissipative Systems Analysis and Control. Theory and Applications*, Springer CCES, London, (2007), 2nd Ed.

[7] Brogliato, B., Niculescu, S.-I., Orhant, P.: *On the control of finite-dimensional mechanical systems with unilateral constraints*, IEEE Trans. Autom. Contr. **42**(2), 200-215, (1997).

[8] Dzonou, R. and Monteiro Marques, M.D.P.:*A sweeping process approach to inelastic contact problems with general inertia operators*, European Journal of Mechanics - A/Solids, **26**(3), 474-490, (2007).

[9] Facchinei, F. and Pang, J.S.: *Finite-dimensional Variational Inequalities and Complementarity Problems*, Springer Series in Operations Research, New-York, (2003).

[10] Galeani, S., Menini, L., Potini, A. and Tornambè, A.: *Trajectory tracking for a particle in elliptical billiards*, International Journal of Control, vol. **81**(2), 189-213, (2008).

[11] Glocker, C.: *Set Value Force Laws: Dynamics of Non-Smooth Systems* Lecture Notes in Applied Mechanics, Vol.1, Springer, (2001).

[12] Glocker, C.: *Concepts for Modeling Impacts without Friction*, Acta Mechanica, Vol. **168**, 1-19, (2004).

[13] Leine, R.I. and van de Wouw, N.: *Stability properties of equilibrium sets of nonlinear mechanical systems with dry friction and impact*, Nonlinear Dynamics, Vol **51**(4), 551-583, (2008).

[14] Mabrouk, M.: *A unified variational model for the dynamics of perfect unilateral constraints*, European Journal of Mechanics A/ Solids, **17**(5), 819-842, (1998).

[15] McClamroch, N. and Wang, D.: *Feedback stabilization and tracking of constrained robots*, IEEE Trans. Autom. Contr. **33**, 419-426, (1988).

[16] Menini, L. and Tornambè, A.: *Asymptotic tracking of periodic trajectories for a simple mechanical system subject to nonsmooth impacts*, IEEE Trans. Autom. Contr. **46**, 1122-1126, (2001).

[17] Menini, L. and Tornambè, A: *Exponential and BIBS stabilisation of one degree of freedom mechanical system subject to single non-smooth impacts*, IEE Proc.-Control Theory Appl. Vol.**148**, No. 2, 147-155, (2001).

[18] Menini, L. and Tornambè, A: *Dynamic position feedback stabilisation of multidegrees-of-freedom linear mechanical system subject to nonsmooth impacts*, IEE Proc.- Control Theory Appl. Vol.**148**, No. 6, 488-496, (2001).

[19] Moreau, J. J: *Unilateral contact and dry friction in finite freedom dynamics*, Nonsmooth Mechanics and Applications, CISM Courses and Lectures, Vol. **302** (Springer-Verlag), (1988).

[20] Sadegh, N. and Horowitz, R.: *Stability analysis of an adaptive controller for robotic manipulators*, IEEE Int. Conference on Robotics and Automation, Vol **4**, 1223- 1229, (1987).

[21] Slotine, J. J. and Li, W.: *Adaptive manipulator control: A case study*, IEEE Trans. Autom. Contr. **33**, 995-1003, (1988).

[22] Hiriart-Urruty J.B and Lemaréchal, C.: *Fundamentals of Convex Analysis*, Springer-Verlag, Grundlehren Texts in Mathematics, (2001).

Centre de recherche INRIA Grenoble – Rhône-Alpes
655, avenue de l'Europe - 38334 Montbonnot Saint-Ismier (France)

Centre de recherche INRIA Bordeaux – Sud Ouest : Domaine Universitaire - 351, cours de la Libération - 33405 Talence Cedex
Centre de recherche INRIA Lille – Nord Europe : Parc Scientifique de la Haute Borne - 40, avenue Halley - 59650 Villeneuve d'Ascq
Centre de recherche INRIA Nancy – Grand Est : LORIA, Technopôle de Nancy-Brabois - Campus scientifique
615, rue du Jardin Botanique - BP 101 - 54602 Villers-lès-Nancy Cedex
Centre de recherche INRIA Paris – Rocquencourt : Domaine de Voluceau - Rocquencourt - BP 105 - 78153 Le Chesnay Cedex
Centre de recherche INRIA Rennes – Bretagne Atlantique : IRISA, Campus universitaire de Beaulieu - 35042 Rennes Cedex
Centre de recherche INRIA Saclay – Île-de-France : Parc Orsay Université - ZAC des Vignes : 4, rue Jacques Monod - 91893 Orsay Cedex
Centre de recherche INRIA Sophia Antipolis – Méditerranée : 2004, route des Lucioles - BP 93 - 06902 Sophia Antipolis Cedex

Éditeur
INRIA - Domaine de Voluceau - Rocquencourt, BP 105 - 78153 Le Chesnay Cedex (France)
http://www.inria.fr
ISSN 0249-6399